A New Generation of Earthquake Recurrence Models Based on The Extreme Value Theory and Impact on Probabilistic Seismic Hazard Assessments

Anne Dutfoy (anne.dutfoy@edf.fr)
EDF Lab Saclay https://orcid.org/0000-0002-5139-106X
Gloria Senfaute
EDF Lab Saclay

Research Article

Keywords: Recurrence model, Probabilistic Seismic Hazard Analysis, Gutenberg-Richter, Extreme Value Theory, Generalized Pareto Distribution

Posted Date: March 15th, 2021

DOI: https://doi.org/10.21203/rs.3.rs-293705/v1

Noname manuscript No.
(will be inserted by the editor)

A New Generation of Earthquake Recurrence Models Based on The Extreme Value Theory and Impact on Probabilistic Seismic Hazard Assessments

Anne DUTFOY, Gloria SENFAUTE

Received: date / Accepted: date

Abstract Probabilistic Seismic Hazard Analysis (PSHA) procedures require that at least the mean activity rate be known, as well as the distribution of magnitudes. Within the Gutenberg-Richter assumption, that distribution is an Exponential distribution, upperly truncated to a maximum possible magnitude denoted m_{max}. This parameter is often fixed from expert judgement under tectonics considerations, due to a lack of universal method.
In this paper, we propose two innovative alternatives to the Gutenberg-Richter model, based on the Extreme Value Theory and that don't require to fix a priori the value of m_{max}: the first one models the tail distribution magnitudes with a Generalized Pareto Distribution; the second one is a variation on the usual Gutenberg-Richter model where m_{max} is a random variable that follows a distribution defined from an extreme value analysis.
We use the maximum likelihood estimators taking into account the unequal observation spans depending on magnitude, the incompleteness threshold of the catalog and the uncertainty in the magnitude value itself. We apply these new recurrence models on the data observed in the Alps region, in the south of France and we integrate them into a probabilistic seismic hazard calculation to evaluate their impact on the seismic hazard levels. The proposed new recurrence models introduce a reduction of the seismic hazard level compared to the common Gutenberg-Richter model conventionally used for PSHA calculations. This decrease is significant for all frequencies below 10 Hz, mainly at the lowest frequencies and for very long return periods. To our knowledge, both new models have never been used in a probabilistic seismic hazard calculation and constitute a new promising generation of recurrence models.

Keywords Recurrence model · Probabilistic Seismic Hazard Analysis · Gutenberg-Richter · Extreme Value Theory · Generalized Pareto Distribution

A. Dutfoy
EDF R&D Saclay Lab
7 Boulevard Monge
91120 Palaiseau
FRANCE
Tel.: +33-1-78194151
E-mail: anne.dutfoy@edf.Fr
G. Senfaute
EDF R&D Saclay Lab
7 Boulevard Monge
91120 Palaiseau
FRANCE
Tel.: +33-1-78193433
E-mail: gloria.senfaute@edf.Fr

1 Introduction

Probabilistic Seismic Hazard Analysis (PSHA) has become a fundamental tool in assessing seismic hazards and seismic input motions to evaluate critical facilities ([2], [3]) and in developping codes at national or regional scale ([15], [19]). Over the last 15 years, the PSHA practice has greatly improved, mainly motivated by research programs launched around the world ([8], [29], [32], [33]).

One important task in PSHA consists of calculating the activity rate for any seismic source and the earthquake magnitude-frequency distribution. The most common model is based on the empirical Gutenberg-Richter law ([20], [21]), defined by:

$$\log \mathbb{E}\left[N_m\right] = a - bm \tag{1}$$

where $\mathbb{E}\left[N_m\right]$ is the mean number of earthquakes whose magnitude is larger than m. Under the asumption that

earthquakes are generated by a stationary Poisson point process, this relation implies that magnitudes are Exponentially distributed. As the total energy released by earthquakes is finite, some deviation from the Gutenberg-Richter straight line is required for large magnitudes: many authors have proposed some improvements ([14], [22], [28], [31], [35]): some of them consist of truncating the Exponential distribution to a regional maximum possible magnitude m_{max} that is the largest possible earthquake of seismic and tectonic setting. For stable continental regions with poor identification of seismogenic structures and low earthquake rates, the determination of m_{max} is a tricky matter. Currently, there is no widely accepted method to estimate m_{max}. One possible way is based on the empirical relationships between the magnitude and various tectonic and fault parameters, such as the fault length or the rupture dimension ([6], [36]). Another possible way is based on records of the largest historic or paleo earthquakes applied especially in areas of low seismicity, where large events have long return periods ([26]). In the absence of any tectonic information, the maximum possible earthquake magnitude is assumed to be equal to the largest magnitude of the catalog, or the largest one plus an increment defined by experts judgement ([37]). Kijko & al have proposed some statistical estimators of the maximum magnitude ([22], [24], [23]) but the author himself admits that these estimations prove to be very near the maximum magnitude of the catalog.

The objective of this paper is to propose two innovative alternatives to the Gutenberg-Richter model, based on the Extreme Value Theory and that doesn't require to fix a priori the value of m_{max}:

- the first model uses a Generalized Pareto Distribution (GPD) to model the tail distribution of magnitudes;
- the second model is a variation on the usual Gutenberg-Richter model: the Exponential distribution is truncated to a random maximum magnitude that follows a distribution resulting from an extreme value analysis.

These new recurrence models are implemented into PSHA in order to check their consistency with the common Gutenberg-Richter model, as well as to assess their impact on seismic hazard levels mainly for long return periods of interest in the nuclear facilities.

The paper is organized as follows. First, we present both innovative recurrence models, after we have reminded the truncated Gutenberg-Richter model (see Sect. 2). Then, we estimate these three recurrence models on a particular seismic region (see Sect. 3). At last, we integrate them into a complete probabilistic seismic hazard calculation to evaluate their impact on the seismic hazard levels (see Sect. 4). Both innovative models constitute a generation of recurrence models that, to our knowledge, has never been used in PSHA.

2 Earthquake Recurrence Models

We present in this section the usual Gutenberg-Richter model and our innovative models, both of them being based on the Extreme Value Theory.
We use the maximum likelihood procedure based on data that show the following main features: 1. observation spans depend on magnitude; 2. magnitudes are considered as imprecise: each magnitude is supposed to uniformly belong to an interval of length 0.5; 3. we don't take into account magnitudes lower than $m_0 = 3.5\, M_w$, supposed to be unreliable.
This last feature implies that we will estimate the restriction of the earthquake Poisson point process to the data range $[m_0, m_{max}]$.

2.1 The Gutenberg-Richter model (GRt-imp)

This model relies on the Gutenberg-Richter law (1), where magnitudes are Exponentially distributed, with a maximum magnitude m_{max} fixed by experts judgement under geophysical considerations. Then, the restriction of the earthquake Poisson point process to the data range $[m_0, m_{max}]$ is defined by:

- the magnitude distribution: Exponential(β) truncated to $[m_0, m_{max}]$,
- the annual counting distribution: Poisson(μ_0) distribution, where μ_0 is the mean annual number of earthquakes with magnitude larger than m_0.

The Gutenberg-Richter parameters (a, b) are linked to (β, μ_0) by:

$$\begin{cases} a = g(\beta, \mu_0) = log_{10}\mu_0 - \log_{10}\left(\dfrac{e^{-\beta m_0} - e^{-\beta m_{max}}}{1 - e^{-\beta m_{max}}}\right) \\ b = f(\beta) = \beta / \log 10 \end{cases} \tag{2}$$

The recurrence model is given for all $m \geq 0$ by:

$$\log \mathbb{E}\left[N_m\right] = a + \log_{10} \frac{10^{-bm} - 10^{-bm_{max}}}{1 - 10^{-bm_{max}}} \tag{3}$$

The maximum likelihood estimator of $(\hat{\beta}, \hat{\mu}_0)$ is detailed in [18], as well as its asymptotic properties. The estimator of (a, b) is defined by :

$$(\hat{a}, \hat{b}) = (g(\hat{\beta}, \hat{\mu}_0), f(\hat{\beta})) \tag{4}$$

$(\hat{\beta}, \hat{\mu}_0)$ is asymptotically Normal. Due to the regularity of f and g, $(\hat{a}, \hat{b})$ is still asymptotically Normal, which allows to determine confidence intervals on a and b.

2.2 The Generalized Pareto Distribution based model (GPD-imp)

This model still relies on the Poisson point process modelization of earthquakes. It is an alternative to the Gutenberg-Richter law (1) as the tail distribution of magnitudes is based on the Extreme Value Theory: the Exponential distribution is not assumed any more and a Generalized Pareto Distribution (GPD) is used to model magnitudes larger than a threshold u, to be determined.

The restriction of the earthquake Poisson point process to magnitudes larger than u is defined by:

- the excesses of magnitudes above u are distributed according to a GPD(σ, ξ),
- the annual counting distribution of magnitudes larger than u follows a Poisson(μ_u), where μ_u is the mean annual number of earthquakes with magnitude larger than u.

A GPD(σ, ξ) is parametered by a scale parameter σ and a shape parameter ξ. Given that the strain energy released in a region is necessarily bounded, the magnitude distribution must be bounded too. Thus, it belongs to the Weibull attraction domain with $\xi < 0$. The cumulated distribution function (cdf) of a GPD where $\xi < 0$ is defined for all $x \in [0, -\frac{\sigma}{\xi}]$ by:

$$H_{\sigma,\xi}(x) = 1 - \left(1 + \xi \frac{x}{\sigma}\right)^{-1/\xi}$$

We denote by $M_0 = M | M \geq m_0$ the magnitudes larger than m_0 and by F_0 its cdf. If u is large enough ([30]), then the tail distribution of M_0 is written for all $m \geq u$ as:

$$\bar{F}_0(m) = \bar{F}_0(u) \bar{H}_{(\sigma,\xi)}(m - u) \tag{5}$$

where $\bar{F}_0 = 1 - F_0$ and $\bar{H}_{(\sigma,\xi)} = 1 - H_{(\sigma,\xi)}$.

The recurrence model is defined for all $m \geq u$ by:

$$\log_{10} \mathbb{E}\left[N_m\right] = \log_{10} \mu_u - \frac{1}{\xi} \log_{10} \left(1 + \xi \frac{m - u}{\sigma}\right) \tag{6}$$

The expression of the maximum likelihood estimator of (σ, ξ, μ_u) is detailed in [16] and [17]. In particular, the estimator is asymptotically Normal, which allows to determine confidence intervals on (σ, ξ, μ_u).

2.3 The Random Gutenberg-Richter model (GRt-al)

The *Random Gutenberg-Richter* model is an innovative variation on the common truncated Gutenberg-Richter model: magnitudes are supposed to be distributed according to an Exponential distribution truncated to a random upper bound magnitude M_{max}. The random upper bound M_{max} follows a distribution $\mathcal{L}_{M_{max}}$ resulting from an extreme value analysis. The model is formally written as:

$$\begin{cases} M | M_{max} \sim \mathcal{E}xp\left(b \log 10\right) \text{ truncated to } [0, M_{max}] \\ M_{max} \quad\quad\quad\quad \sim \mathcal{L}_{M_{max}} \end{cases}$$

where b is the usual Gutenberg-Richter parameter, estimated in *The Gutenberg-Richter model (GRt-imp)* Section. It is important to note that the estimation of b is independent of the upper bound of the Exponential, which allows to estimate it in a separate way.

The distribution $\mathcal{L}_{M_{max}}$ is the result of an extreme value analysis of magnitudes: we consider the asymptotic distribution of the estimator of a well-chosen quantile of large order of M_0.
The quantile q_p of order p is defined by $F_0(q_p) = p$, and from (5), with $\zeta_u = \bar{F}_0(u)$ and $\xi < 0$, we deduce that:

$$q_p = u + \frac{\sigma}{\xi} \left[\left(\frac{1 - p}{\zeta_u} \right)^{-\xi} - 1 \right] \tag{7}$$

We denote by g_p the function such that $q_p = g_p(\sigma, \xi)$ and we consider the estimator $\hat{q}_p$ of q_p:

$$\hat{q}_p = g_p(\hat{\sigma}, \hat{\xi}) \tag{8}$$

We know that $(\hat{\sigma}, \hat{\xi})$ is asymptotically Normal, with a covariance matrix denoted $\boldsymbol{\Sigma}$. Under regularity considerations, we deduce that $\hat{q}_p$ is also a maximum likelihood estimator, asymptotically Normal, with covariance matrix $\boldsymbol{\Gamma}$ that is written as:

$$\boldsymbol{\Gamma} = \nabla g_p(\hat{\sigma}, \hat{\xi}) \boldsymbol{\Sigma} \nabla g_p(\hat{\sigma}, \hat{\xi})^\top \tag{9}$$

where $\nabla g_p(\hat{\sigma}, \hat{\xi}) = (\frac{\partial g_p}{\partial \sigma}(\hat{\sigma}, \hat{\xi}), \frac{\partial g_p}{\partial \xi}(\hat{\sigma}, \hat{\xi}))$. From relation (7), we have:

$$\frac{\partial g_p}{\partial \sigma}(\sigma, \xi) = \frac{1}{\xi} \left[\left(\frac{1 - p}{\zeta_u} \right)^{-\xi} - 1 \right]$$

$$\frac{\partial g_p}{\partial \xi}(\sigma, \xi) = -\frac{\sigma}{\xi} \left[\frac{1}{\xi} + \log \left(\frac{1 - p}{\zeta_u} \right) \right] \left(\frac{1 - p}{\zeta_u} \right)^{-\xi} + \frac{\sigma}{\xi^2}$$

which enables to determine $\boldsymbol{\Gamma}$ and finally the asymptotic distribution of $\hat{q}_p$.

Furthermore, it is very important to take into account the maximum magnitude $m_{max,cat}$ of the catalog: it would be nonsense that M_{max} be lesser than $m_{max,cat}$.Thus, $\mathcal{L}_{M_{max}}$ has to be truncated to the lower bound $m_{max,cat}$ to ensure that M_{max} be larger than $m_{max,cat}$ with a probability equal to 1.

It is worth noting that the cdf F of magnitudes is related to F_0 through the relation $\bar{F}(m) = \zeta_u \bar{F}_0(m)$ for all $m \geq u$. Then, we have $F(q_p) \geq F_0(q_p)$, implies

that q_p is indeed a F-quantile of order $\tilde{p} \geq p$. In other words, q_p is a more extreme value with respect to the distribution F than with respect to the F_0 distribution.

We want to emphasize that assigning to M_{max} the distribution of the GPD(σ, ξ) upper bound: $u - \hat{\sigma}/\hat{\xi}$ deduced from the Normal asymptotic distribution of $(\hat{\sigma}, \hat{\xi})$ would not be a good idea, due to the irregularity of the function $(\sigma, \xi) \to u - \sigma/\xi$ at any point of kind $(\sigma, 0)$: any small variation on ξ induces a large variation on the upper bound. Thus, uncertainty on ξ induces a huge variance in the distribution of $u - \sigma/\xi$. On the contrary, the estimation of any quantile of large order is much more stable as the function g_p is infinitely regular at any point of kind $(\sigma, 0)$ (for example, the derivability at $(\sigma, 0)$ is ensured by the equivalent $\partial g/\partial \xi(\sigma, \xi) \sim (1/2)\sigma \log^2 \alpha$ with $\alpha = \zeta_u(1-p)$).
More generally, the upper bound of a distribution gives poor information on its extreme values and the decreasing speed of its tail is more informative. Consider, for example, the Normal and LogNormal distributions: both ones have an infinite upper bound whereas the probability to be farther than 4 standard deviations from the mean is about 10^{-5} for the Normal distribution and 10^{-2} for the LogNormal one. The study of large order quantiles is more significant: the quantile of order 99% is 2.33 standard deviations from the mean for the Normal distribution, while it is 4.9 standard deviations for the LogNormal one.

2.4 Models comparison

To help the comparison, we detail in this section the pros and cons of each model.

The truncated Gutenberg-Richter model is an improvement with respect to the Gutenberg-Richter model (1) as the frequency-magnitude curve falls off from the straight line when the magnitude increases. The difficulty remains in the choice of m_{max}, on which the recurrence model strongly depends and that raises debates among the seismologist community.

The GPD-based model is an improvement with respect to the truncated Gutenberg-Richter model (3) as the frequency-magnitude curve falls off from the straight line when the magnitude increases whithout any additional hypothesis on the maximum possible magnitude: its upper bound results from the GPD estimation, equal to $m_{max} = u - \sigma/\xi$ if $\xi < 0$.

However, for areas with low seismicity, the estimation of the GPD-based model might be tricky, due to the eventual low number of earthquakes in stable continental regions and particularly earthquakes with large magnitude.

Compared to the previous models, the Random Gutenberg-Richter model presents the following advantages: 1. It requires less data to be estimated: indeed, the GPD-based model needs enough data to assume that the empirical tail distribution has converged towards an extreme value distribution, whereas the Random Gutenberg-Richter model estimates the Exponential parameters using all the available data (and not only the largest ones); 2. It is able to model the uncertainty of the upper troncature thanks to an extreme value analysis. In domains where the seismicity is low, that feature proves to be essential.

To conclude, it is worth considering the following good practices: for domains of high seismicity, if no value m_{max} achieves universal agreement, the GPD-based model is likely to help to model the tail distribution whithout any additional hypothesis. For domains of low seismicity, the Random Gutenberg-Richter model should be used after the random modelisation of m_{max} has been done on a larger domain thanks to the GPD-based model. In general, the simultaneous use of all the models help to better understand their respective limitations and their impact on hazard assessments.

3 Application To The Alps Region, France

3.1 The Alps data

In this section, we apply the whole approach to the mountain region Alps, in the south of France, that is one of the most active regions in France. A homogenous seismotectonic zone was delimited based on geological, structural, geophysical, neotectonic and seismological data. We use the FCAT17 catalog ([25]) (see Data and Resources Section) that gathers recent instrumental magnitudes measured by seismometers ([10], [11]) and magnitudes attributed to historical events ([1]). Magnitudes were derived from historical documents ([34] , [33]) in a 2-step process: 1. The historical information was translated into Intensities, and 2. Magnitudes were derived from Intensity maps. All magnitudes are given in M_w. Figure 1 presents the location of earthquakes inside of the delimited seismotectonic domain earthquakes.

A declustering method was applied to separate the time-dependent part of seismicity from the seismic activity related to aftershocks, foreshocks or clusters of earthquakes.

Complete periods associated to each class of magnitudes are defined Table 1. Furthermore, we left all besides the magnitudes lower than $m_0 = 3.5M_w$, considered as not reliable. We assume that the restricted catalog constitutes a complete statistical sample. Our

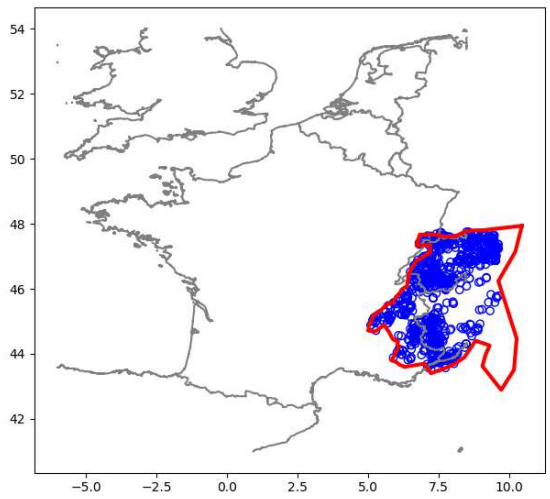

Fig. 1 Earthquakes in the Alps in France (longitude - latitude units).

Table 1 Complete periods for each class of magnitude, in years.

Magnitude class (M_w)	Complete period
$[3.5, 4]$	$[1850, 2016]$
$[4, 4.5]$	$[1850, 2016]$
$[4.5, 5]$	$[1700, 2016]$
$[5, 5.5]$	$[1600, 2016]$
≥ 5.5	$[1500, 2016]$

database finally contains $N = 583$ earthquake events, from year 1524 until year 2016, whose magnitudes range from 3.5 until 6.69. The database is large enough to achieve robust results with all the models presented.

Furthermore, the accuracy of magnitude data can sometimes be no better than 0.5 unit: this can be due to imprecise measurement methods or to bias introduced when converting from various local magnitude scales. In this case, we can't account for the precise value of the magnitude to fit our models: only that is belongs to C_i length 0.5.

We used the open source software OpenTURNS [7] to perform the probabilistic calculus that provides advanced probabilistic modelizations and statistical functionalities.

3.2 The Gutenberg-Richter model (GRt-imp)

The maximum magnitude selected for the region is $m_{max} = 7.5\,M_w$, based on tectonic information and expert opinion. Using the maximum likelihood estimators, we obtained:

$$\begin{cases} \hat{a} = 3.87 \\ \hat{b} = 0.965 \end{cases}$$

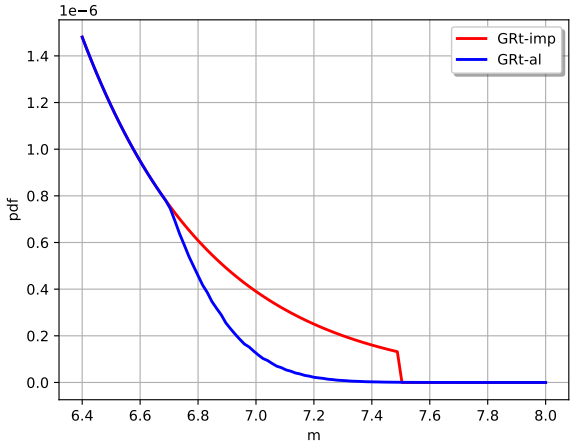

Fig. 2 Distribution of magnitudes: Exponential($\hat{b}\log 10$) truncated to $m_{max} = 7.5\,M_w$ (*GRt-imp*) or to the random variable $M_{max} \sim \mathcal{N}(\mu = 6.75\,M_w, \sigma^2 = 7.63\,10^{-2})$ truncated to $[6.69\,M_w, +\infty[$ (*GRt-al*).

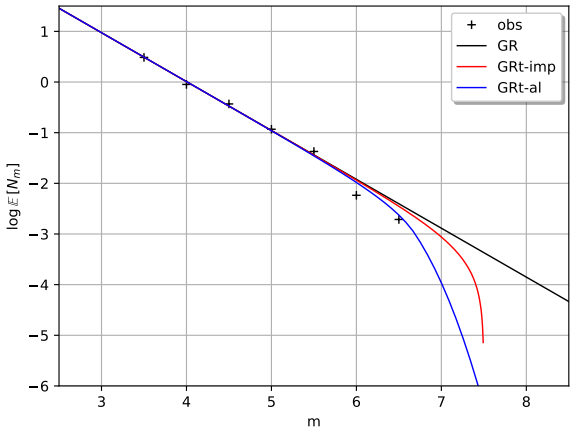

Fig. 3 Recurrence model associated to the Exponential($\hat{b}\log 10$) truncated to $m_{max} = 7.5\,M_w$ (*GRt-imp*); or to the random variable $M_{max} \sim \mathcal{N}(6.75\,M_w, 7.63\,10^{-2})$ truncated to $[6.69\,M_w, +\infty[$ (*GRt-al*).

Figures 2 and 3 respectively draw in red the distribution of magnitudes and the associated recurrence models compared to the Gutenberg-Richter straight line.

The asymptotic distribution of $(\hat{b}, \hat{a})$ is Normal whith mean and covariance matrix:

$$(\hat{b}, \hat{a}) \sim \mathcal{N}\left(\begin{bmatrix} 0.965 \\ 3.87 \end{bmatrix}, \boldsymbol{\Sigma} = \begin{bmatrix} 1.03\,10^{-3} & 3.72\,10^{-3} \\ 3.72\,10^{-3} & 1.38\,10^{-2} \end{bmatrix} \right) \quad (10)$$

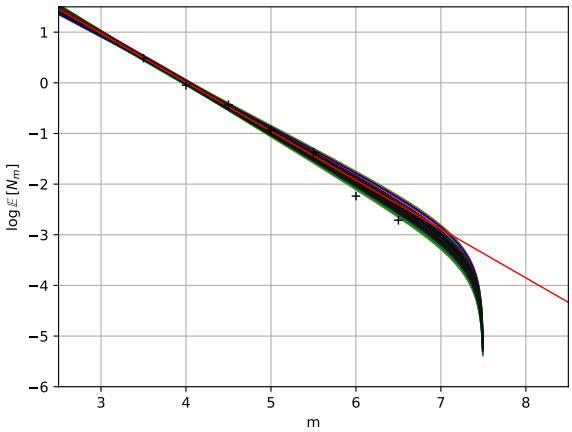

Fig. 4 *GRt-imp*: Uncertainties on $(\hat{b}, \hat{a})$: 100 possible recurrence models.

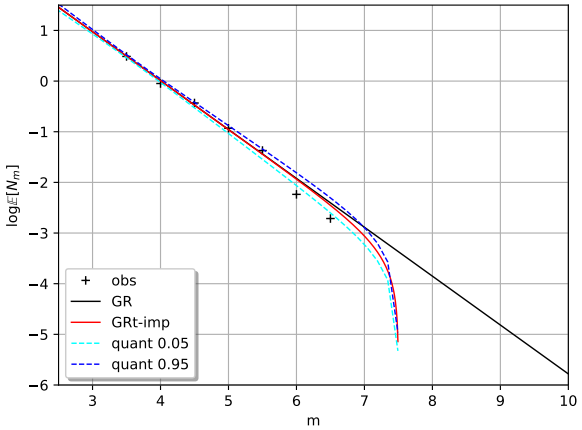

Fig. 5 *GRt-imp*: uncertainties on the recurrence model due to uncertainties on $(\hat{b}, \hat{a})$: quantile curves of level 5% and 95%, built from 10^6 models.

Using the margins of (10), we can define confidence intervals of level 90% for a and b:

$$\begin{cases} \mathbb{P}\left[a \in [3.68, 4.06]\right] &= 0.9 \\ \mathbb{P}\left[b \in [0.912, 1.02]\right] &= 0.9 \end{cases} \tag{11}$$

Generating a sample of (b, a) from (10) allows to draw all the corresponding recurrence models and thus visualize the impact of the estimation uncertainty of (b, a) on the recurrence model. Figure 4 shows 100 generated recurrence models and Figure 5 shows the 5% and 95% quantile curves, built from 10^6 models. Table 2 details some values of the quantile curves. We note that the mean annual number of earthquakes whose magnitude is larger than 7 is less than $1.11\,10^{-3}$ with a 95% probability.

Among several tests to validate the fitted Poisson point process, we focus here on the good fitting of the

Table 2 *GRt-imp* model: Uncertainties on $\mathbb{E}\left[N_m\right]$ induced by uncertainties on $(\hat{b}, \hat{a})$: 5% quantile, 95% quantile and median of $\mathbb{E}\left[N_m\right]$.

$m\,(M_w)$	$\mathbb{E}\left[N_m\right]$ 5% Quant.	50% Quant.	95% Quant.
3.5	3.25	3.49	3.75
4	$8.46\,10^{-1}$	$9.22\,10^{-1}$	1.00
4.5	$2.99\,10^{-1}$	$3.39\,10^{-1}$	$3.84\,10^{-1}$
5	$1.05\,10^{-1}$	$1.25\,10^{-1}$	$1.48\,10^{-1}$
5.5	$2.56\,10^{-2}$	$2.3.26\,10^{-2}$	$4.14\,10^{-2}$
6	$8.78\,10^{-3}$	$1.17\,10^{-2}$	$1.56\,10^{-2}$
6.5	$2.89\,10^{-3}$	$4.05\,10^{-3}$	$5.66\,10^{-3}$
7.0	$5.10\,10^{-4}$	$7.54\,10^{-4}$	$1.11\,10^{-3}$

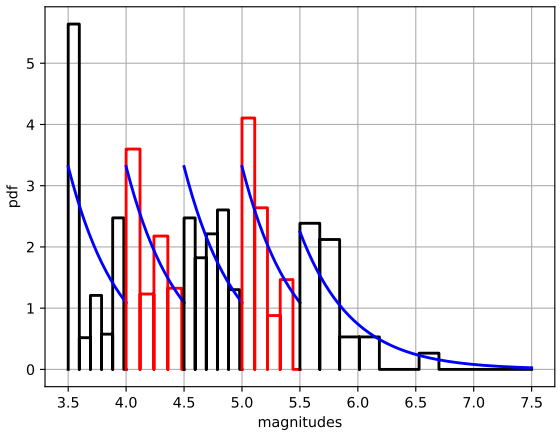

Fig. 6 *GRt-imp*: Validation of the magnitudes distribution: empirical and estimated distributions of $M|M \in \mathcal{C}_k$ for each class $\mathcal{C}_k$.

estimated distribution of magnitudes on data: it consists of drawing the estimated distribution of $M|M \in \mathcal{C}_k$, where $\mathcal{C}_k$ is a class of magnitudes, and the empirical cumulative rates in the same plot: Figure 6 shows that the fitting is correct.

3.3 The Generalized Pareto Distribution based model (GPD-imp)

We first determined the threshold u thanks to different modelizations of the distribution of $M_0 = M|M \geq m_0$: non parametric fitting with normal or uniform kernels. We fixed $u = 4.0$ that is a quantile of order larger than 80%. Using the maximum likelihood estimators, we obtained:

$$\begin{cases} \hat{\sigma} &= 0.586 \\ \hat{\xi} &= -0.143 \\ \hat{\mu}_u &= 0.900 \end{cases} \tag{12}$$

Figure 7 shows the tail distribution of magnitudes M_0, for magnitudes larger than $u = 4.0$. Figure 8 shows

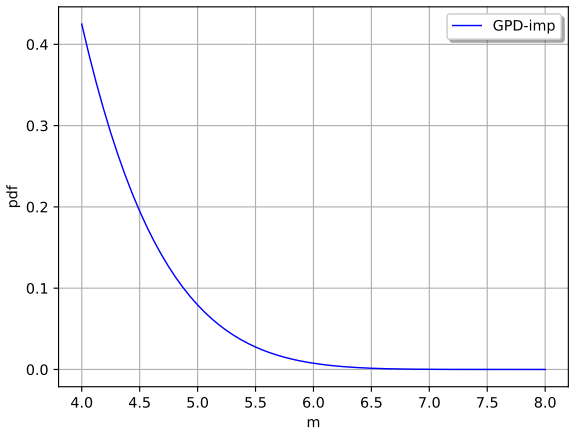

Fig. 7 *GPD-imp*: Tail distribution of magnitudes $M_0 = M|M \geq m_0$ based on the Generalized Pareto Distribution GPD$(\hat{\sigma}, \hat{\xi})$ for magnitudes larger than $u = 4.0\, M_w$.

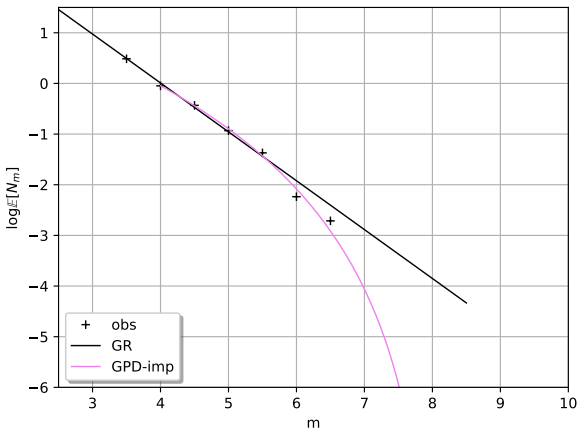

Fig. 8 *GPD-imp*: Recurrence model associated to the GPD$(\hat{\sigma}, \hat{\xi})$ tail distribution for magnitudes larger than $u = 4.0\, M_w$ and the $\mathcal{P}(\hat{\mu}_u)$ counting distribution.

the associated recurrence model, compared to the Gutenberg-Richter line.

The asymptotic distribution of $(\hat{\sigma}, \hat{\xi}, \hat{\mu}_u)$ is Normal with mean and covariance matrix:

$$(\hat{\sigma}, \hat{\xi}, \hat{\mu}_u) \sim \mathcal{N}\left(\begin{bmatrix} 0.586 \\ -0.143 \\ 0.900 \end{bmatrix}, \boldsymbol{C} \right) \tag{13}$$

where

$$\boldsymbol{C} = \begin{bmatrix} 2.50\,10^{-3} & -2.10\,10^{-3} & -1.06\,10^{-3} \\ -2.10\,10^{-3} & 2.52\,10^{-3} & 6.72\,10^{-4} \\ -1.06\,10^{-3} & 6.72\,10^{-4} & 4.18\,10^{-3} \end{bmatrix} \tag{14}$$

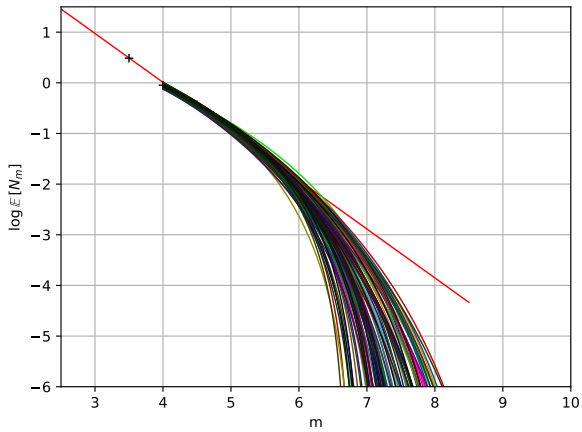

Fig. 9 *GPD-imp*: Uncertainties on $(\hat{\sigma}, \hat{\xi}, \hat{\mu}_u)$: 100 possible recurrence models.

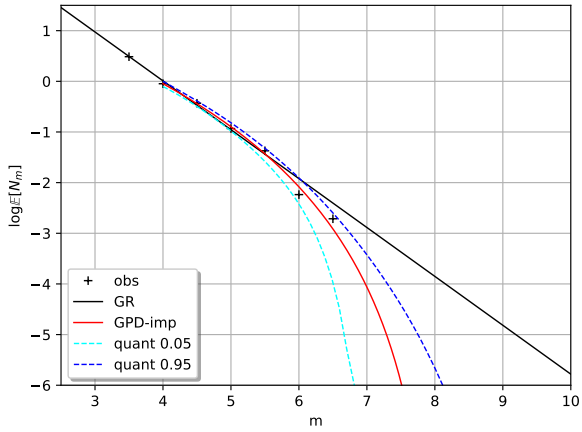

Fig. 10 *GPD-imp*: Uncertainties on the recurrence model due to uncertaintes on $(\hat{\sigma}, \hat{\xi}, \hat{\mu}_u)$: quantile curves of level 5% and 95%, built from 10^6 models.

Using the margins of (13), we can define confidence intervals of level 90% for σ, ξ and μ_u:

$$\begin{cases} \mathbb{P}\left[\sigma \in [0.503, 0.668]\right] & = 0.9 \\ \mathbb{P}\left[\xi \in [-0.226, -0.0608]\right] & = 0.9 \\ \mathbb{P}\left[\mu_u \in [0.794, 1.00]\right] & = 0.9 \end{cases}$$

Generating a sample of (σ, ξ, μ_u) from (13) allows to draw all the corresponding recurrence models and thus visualize the impact of the estimation uncertainty of (σ, ξ, μ_u). Figure 9 shows 100 generated recurrence models and Figure 10 shows the quantile curves of level 5% and 95% built from 10^6 models. Table 3 details some values of the quantile curves. We note that the mean annual number of earthquakes whose magnitude is larger than 7 is less than $3.37\,10^{-4}$ with a probability of 95%.

Table 3 *GPD-imp* model: Uncertainties on $\log \mathbb{E}[N_m]$ induced by uncertainties on $(\hat{\sigma}, \hat{\xi}, \hat{\mu}_u)$: 5% quantile, 95% quantile and median of $\mathbb{E}[N_m]$.

$m\,(M_w)$	$\mathbb{E}[N_m]$ 5% Quant.	50% Quant.	95% Quant.
4.0	$7.91\,10^{-1}$	$8.96\,10^{-1}$	1.00
4.5	$2.94\,10^{-1}$	$3.36\,10^{-1}$	$3.80\,10^{-1}$
5	$1.11\,10^{-1}$	$1.36\,10^{-1}$	$1.61\,10^{-1}$
5.5	$2.50\,10^{-2}$	$3.49\,10^{-2}$	$4.62\,10^{-2}$
6	$4.89\,10^{-3}$	$6.22\,10^{-3}$	$1.45\,10^{-2}$
6.5	$1.25\,10^{-4}$	$1.03\,10^{-3}$	$2.65\,10^{-3}$
7.0	$4.06\,10^{-8}$	$5.02\,10^{-5}$	$3.37\,10^{-4}$
7.5	$7.28\,10^{-11}$	$2.8\,10^{-6}$	$4.73\,10^{-5}$

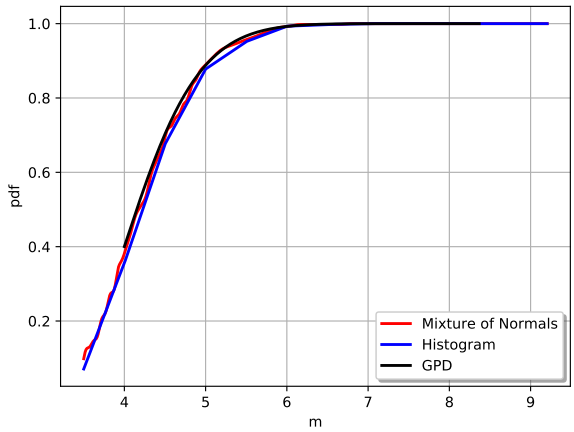

Fig. 11 *GPD-imp*: Validation of the annual maximum magnitudes distribution.

Among several tests to validate the fitted model, we focus here on the good fitting of the annual maximum magnitude distribution whose cdf G is defined by:

$$G(m) = e^{-\mu_u \bar{H}_{(\sigma,\xi)}(m)}, \quad \forall m \geq u \tag{15}$$

The cdf is defined from the estimated GPD model and from a non parametric kernel smoothing with normal or uniform kernels. Figure 11 shows that the fitting is correct.

Besides, Figure 12 shows the estimated annual counting distribution of earthquakes $\mathcal{P}(\hat{\mu}_u)$ with magnitudes larger than $u = 4$ and the empirical one.

3.4 The Random Gutenberg-Richter model (GRt-al)

To elaborate the Random Gutenberg-Richter model, we considered the distribution of the quantile of order $(1 - 10^{-4})$ of the *GPD-imp* model to randomize the upper bound of the Exponential distribution. From (8) and (12), we obtained the estimation $\hat{q}_N$:

$$\hat{q}_N = 6.75\, M_w$$

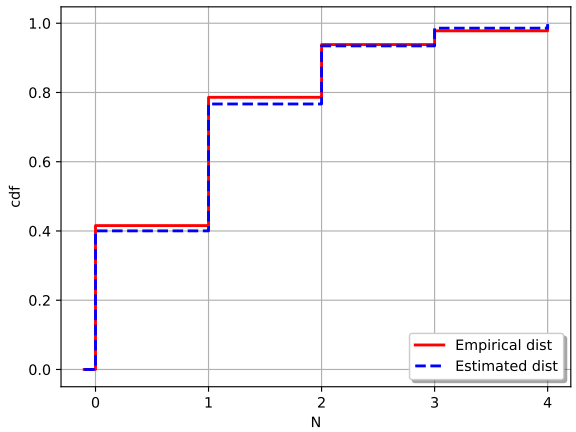

Fig. 12 *GPD-imp*: Validation of the annual counting distribution of earthquakes with magnitudes larger than $u = 4.0\, M_w$.

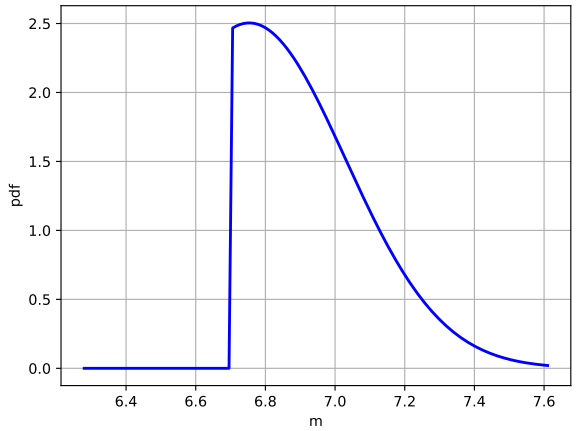

Fig. 13 *GRt-al*: Distribution of the random upper bound M_{max} of the Exponential distribution of magnitudes.

Its asymptotic distribution is Normal, with mean 6.75 and variance $7.63\,10^{-2}$ calculated from (9), that we truncated to the lower bound equal to the maximum magnitude contained in the catalog $m_{max,cat} = 6.69\, M_w$:

$$M_{max} \sim \mathcal{N}(6.75\, M_w, 7.63\,10^{-2}) \tag{16}$$

$$\text{truncated to } [6.69\, M_w, +\infty[\tag{17}$$

Figure 13 shows the pdf of the distribution of $\hat{q}_N$.

Figure 2 shows the final distribution of magnitudes and Figure 3 shows the associated recurrence model compared to the Gutenberg-Richter straight line.

3.5 Results comparison

In this section, we want compare between the previous models: Figure 14 shows the pdf of the conditional

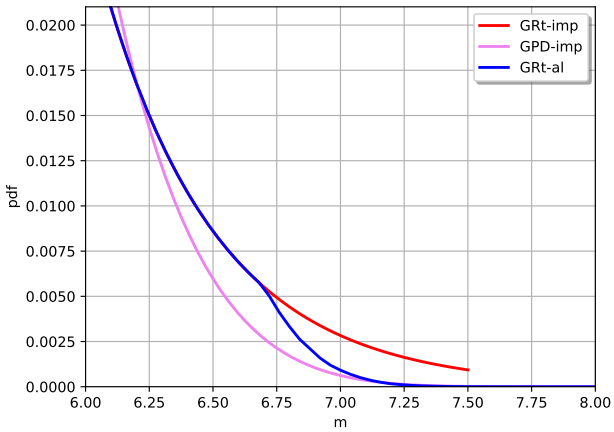

Fig. 14 Distribution of $M_u = M|M \geq u$ based on the Exponential distribution truncated to $m_{max} = 7.5\,M_w$ (*GRt-imp*), on the Exponential distribution truncated to the random magnitude M_{max} (*GRt-al*) or based on the extreme value distribution GPD (*GPD-imp*): zoom on magnitudes larger than $6.0\,M_w$.

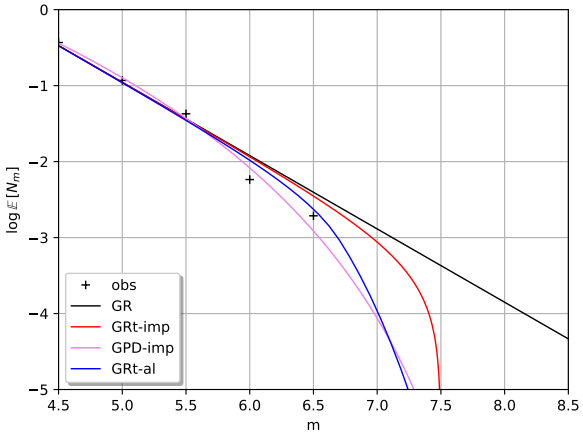

Fig. 15 Recurrence models based on the Exponential distribution truncated to $m_{max} = 7.5\,M_w$ (*GRt-imp*), on the Exponential distribution truncated to the random magnitude M_{max} (*GRt-al*) or based on the extreme value distribution GPD (*GPD-imp*), compared to the Gutenberg-Richter straight line.

magnitude $M_u = M|M \geq u$. We observe that the Random Gutenberg-Richter model appears as a compromise between the classical Gutenberg-Richter model and the GPD-based model as it behaves as the classical Gutenberg-Richter model below the magnitude $6.69\,M_w$ and as the GPD-based model above this threshold.

Figure 15 shows all the recurrence models. Table 4 details some values of the recurrence models at different magnitudes.

Table 4 Recurrence models: mean annual number of earthquakes wich magnitude is larger than m.

$m\,(M_w)$	$\mathbb{E}[N_m]$ *GRT-imp*	*GPD-imp*	*GRT-al*
6.0	$1.16\,10^{-2}$	$8.26\,10^{-3}$	$1.04\,10^{-2}$
6.5	$3.52\,10^{-3}$	$1.22\,10^{-3}$	$2.36\,10^{-3}$
7.0	$8.72\,10^{-4}$	$8.67\,10^{-5}$	$1.09\,10^{-4}$
7.5	0.0	$1.16\,10^{-6}$	$4.06\,10^{-7}$

We note that the truncated Gutenberg-Richter model has the heaviest tail distribution, while the GPD-based model has the slightest one (the pdf of *GRt-imp* is above the pdf of *GPD-imp*). It means that large magnitudes have a higher probability to appear with the truncated Gutenberg-Richter model than with the GPD-based model, even if the upper bound of the GPD-based model is larger thant $m_{max} = 7.5$ fixed to the truncated Gutenberg-Richter model. Once more, the Random Gutenberg-Richter model appears as a compromise as it is equivalent to the truncated Gutenberg-Richter model until the magitude $m_{max,cat} = 6.69$ and then is equivalent to the GPD-based model for larger magnitudes.

4 Probabilistic Seismic Hazard Assessment

In this section, we integrate our innovative recurrence models into a probabilistic seismic hazard calculation in order to check their consistency with the truncated Gutenberg-Richter commonly used in PSHA as well as to assess their impact on probabilistic seismic hazard assessments.

4.1 Methodology

The PSHA computational model used in this study corresponds to Cornell's approach ([13].) This approach calculates the probability of exceeding a target value of ground motion, during a fixed period of time. A probabilistic seismic hazard calculation takes into account the influence of all seismic sources able to contribute to the hazard, as well as the spatial and temporal distribution of the seismicity of each of these sources. Four main steps are necessary to perform a PSHA calculation:

1. Identification of the area seismic sources that might affect the site of interest. Area source models are often used when one cannot identify a specific fault. Usually, in PSHA, a uniform seismicity distribution is assigned to each area source, implying that earthquakes are equally likely to occur at any point within the source zone.

2. Specification of temporal and magnitude seismicity distributions for each source. Cornell's approach assumes that earthquakes follow a Poisson point process. The most commonly used frequency-magnitude model is the Gutenberg-Richter relationship (1).
3. Calculation of ground motions and their uncertainty. Ground Motion Prediction Equations (GMPE) are used to predict the ground motion at the site itself. The parameters of interest include different intensity measures (peak ground acceleration, peak ground velocity, peak ground displacement, spectral acceleration, intensity, strong ground motion duration). Most GMPE available today are empirical and depend on the earthquake magnitude, source-to-site distance, type of faulting and local site conditions.
4. Integration of uncertainties on earthquake location, magnitude and GMPE.

The ultimate result of a PSHA calculation is a seismic hazard curve giving the annual probability of exceeding a specified ground motion parameter. Conceptually, the computation of the seismic hazard is relatively simple, as the calculation is carried out with the following equation:

$$\lambda(IM > x) = \lambda(M > m_{min}) \times \iint \mathbb{P}\left[IM > x | (m, r, \boldsymbol{\theta})\right] f_{M|M>m_{min}}(m) f_R(r)\, dm\, dr \quad (18)$$

where IM is the Intensity Measure of the ground motion parameter; x is the target intensity; $\lambda(IM > x)$ is the annual rate of earthquakes leading to an exceess of the target; $\lambda(M > m_{min})$ is the annual rate of earthquakes of magnitude M larger than the minimum magnitude m_{min} selected for the source zone; $f_{M|M>m_{min}}$ and f_R are the pdf of the magnitude and the distance from the source zone; $\mathbb{P}\left[IM > x | (m, r, \boldsymbol{\theta})\right]$ is the probability that an earthquake of magnitude m at the distance r from the site generates an intensity larger than x; $\boldsymbol{\theta}$ regroups all the other fixed parameters regarding the site, the type of faults, ... This probability is determined using a model of GMPE that takes into account the model errors due to amplifications and misunderstandings of geological phenomena.

The structure of a PSHA calculation is summarized in Figure 16. In the study, the PSHA model is a simplified but realistic model composed of only one area source. It uses real data (see Date and Resources Section) and a conceptual calculation model respecting the international rules. The tool used for the calculations is OpenQuake [27].

The PSHA calculations take into account the following epistemic uncertainties:

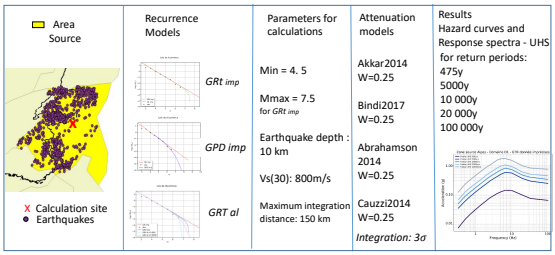

Fig. 16 PSHA structure recurrence models (truncated Gutenberg Richter model (*GRt-imp*), Generalized Pareto Distribution model (*GPD-imp*) and Random Gutenberg Richter model (*GRt-al*)); in yellow the area source definition, in red the site for seismic hazard evaluation; parameters for calculation and attenuation models selected.

- Ground motion models uncertainty: we selected four Ground Motion Prediction Equations (GMPE) . These independent GMPEs are representative of all published database for shallow continental active regions ([4], [5], [9], [12]).
- Maximum magnitude uncertainty: both innovative models *GPD-imp* and *GRt-al* can model this uncertainty, indirectly through the asymptotic distribution of the parameter estimators for the *GPD-imp*, or directly with the distribution of the random upper bound for the *GRt-al* model.
- Recurrence parameters uncertainty: this epistemic uncertainty is taken into account thanks to the asymptotic distribution of the parameter estimators that enables to generate several possible sets of parameters: (a, b) for the Gutenberg-Richter based models and (σ, ξ, μ_u) for the *GPD-imp* model. Each set of parameters thus constitutes an alternative branch of the logic tree.

The final logic-tree of PSHA calculations is composed of 400 branches sum up on Figure 17, each one associated to some specific probabilistic hypotheses. The weights of the logic-tree branches are defined according to the degree of confidence that is given to each of the assumptions and interpretations. In our study, all the branches have the same weight.

4.2 Results and Discussion

Impact of the new generation of recurrence models on the probabilistic seismic hazard We calculate the seismic hazard curves and Uniform Hazard Spectrum (UHS) using the previous recurrence models.

Figure 18 shows all the hazard curves and shows that for all spectral accelerations the curves look sim-

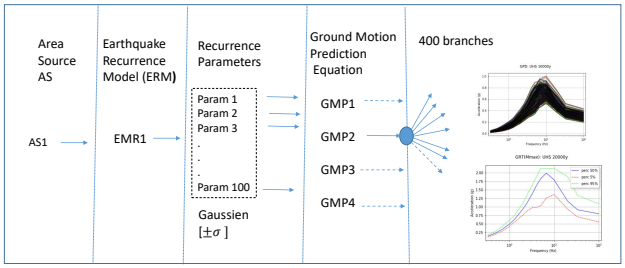

Fig. 17 Logic-tree used to perform PSHA calculations, the model is made of 400 branches.

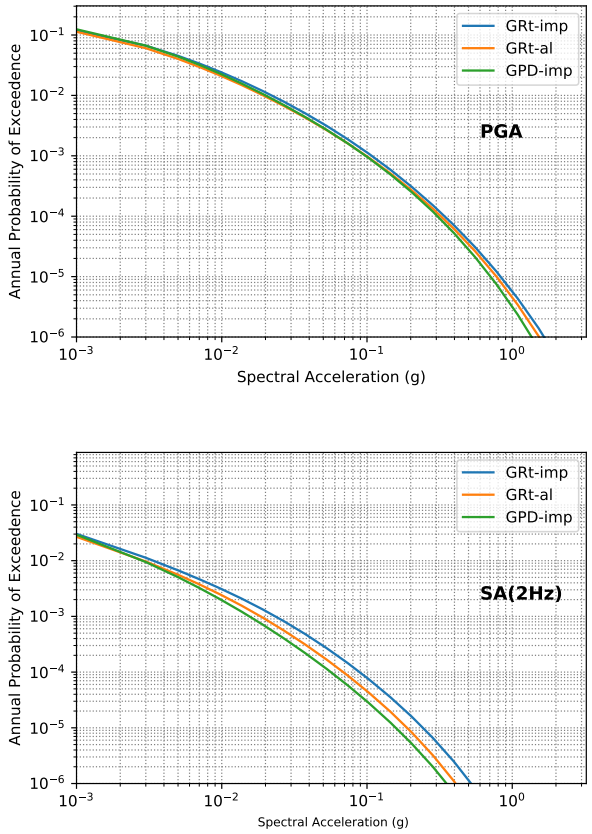

Fig. 18 Comparison of the seismic hazard curves between the new recurrence models: Random Gutenberg-Richter *GRt-al*, Generalized Pareto Distribution *GPD-imp*, and the common Gutenberg Richter model *GRt-imp*, for spectral accelerations PGA and 2 Hz.

ilar: a decrease in the hazard calculated with the new recurrence models (*GRt-al* and *GPD-imp*) compared to the common truncated Gutenberg Richter model (*GRt-imp*). This difference is higher for low frequencies, as it is clearly observed for the spectral period of 2 Hz.

Figure 19 illustrates the impact of the new recurrence models on the UHS calculated for the return periods: 475, 10 000, 20 000 and 100 000 years. This impact is particularly important for low frequencies (below around 10Hz), which is consistent with the impact observed on the seismic hazard curves. This decrease is accentuated for larger return periods, clearly visible for the 100 000 year return period.

Figure 20 quantifies the relative differences of the seismic hazard generated by the new recurrence models with respect to the common truncated Gutenberg-Richter model. The curves show a clear truncation at about 10 Hz: below 10 Hz, there is a marked decrease in the seismic hazard with both new recurrence models, as follows:

- for return periods larger than 5 000 years, the decrease in the seismic hazard of the Generalized Pareto Distribution based model *GPD-imp* is estimated at around 50, 30, 25 and 10% for frequencies 0.5, 1, 2 and 10 Hz respectively with respect to the common truncated Gutenberg-Richter model *GRt-imp*;
- for return periods larger than 5000 years, the decreasing in the seismic hazard of the Random Gutenberg-Richter model*GRt-al* is estimated at about 25, 18, 12 and 5 % for frequencies of 0.5, 1, 2 and 10 Hz respectively with respect to *GRt-imp*.
- for frequencies above 10Hz and up to 100Hz, the reduction in seismic hazard of the *GPD-imp* and *GRt-al* is less than 10% with respect to *GRt-imp*.

We explain that significant decrease by the different modelisations of the extreme magnitudes: the tail distribution of magnitudes of both *GPD-imp* and *GRt-al* is much lighter than the tail of *GRt-imp*, as drawn on Figure 14. The pdf of the innovative models drops towards 0 faster than the pdf of the truncated Gutenberg-Richter model. In particular, the probability to exceed a magnitude equal to $7\,M_w$ calculated from *GPD-imp* and *GRt-al* is 8 times lesser than the probability calculated from *GRt-imp*. That feature is noticeable on the values of the recurrence models: the mean annual number of earthquakes with magnitude larger than $7\,M_w$ is $\mathbb{E}[N_7] = 8.72\,10^{-4}$ with *GRt-imp* model, $\mathbb{E}[N_7] = 1.09\,10^{-4}$ with *GRt-al* and $\mathbb{E}[N_7] = 0.867\,10^{-4}$ with *GPD-imp*.
We insist on the fact that even if the maximum possible magnitude estimated by the GPD-based model, equal to $8.06\,M_w$, is larger than the $m_{max} = 7.5$ fixed by experts to the truncated Gutenberg-Richter model, the GPD-based model gives less weight to large magnitudes than the truncated Gutenberg-Richter model. We have the same feature for the *GRt-al* model whose maximum possible magnitude is theoretically infinite, but whose probability to exceed the magnitude $7\,M_w$ is $1.47\,10^{-8}$.
Thus, these new recurrence models reduce the population of earthquakes with larger magnitudes included in

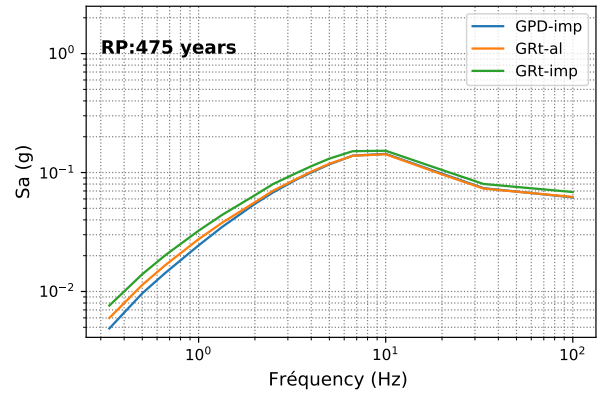

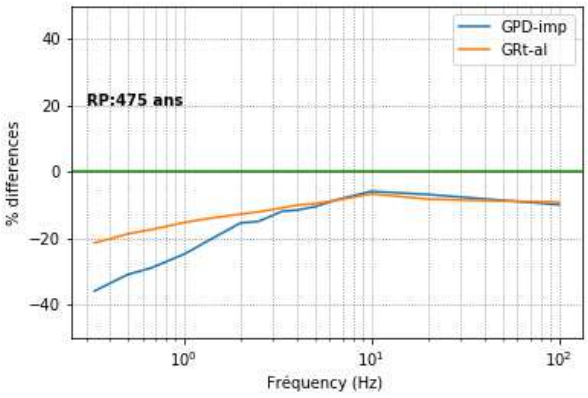

R

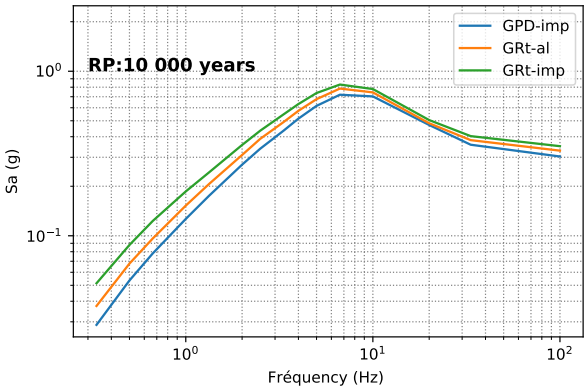

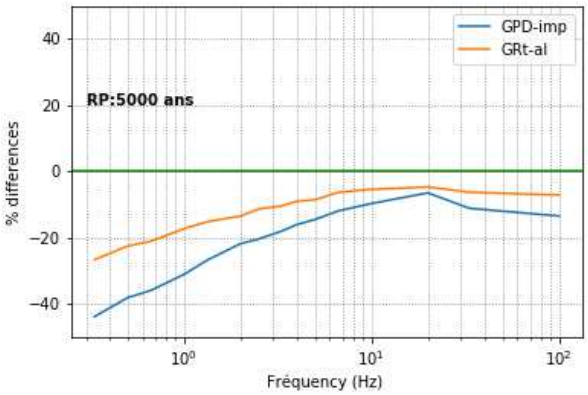

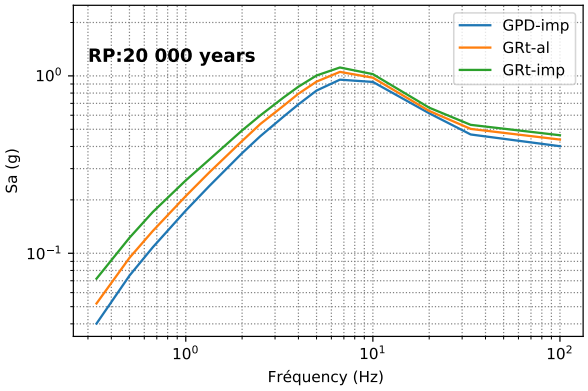

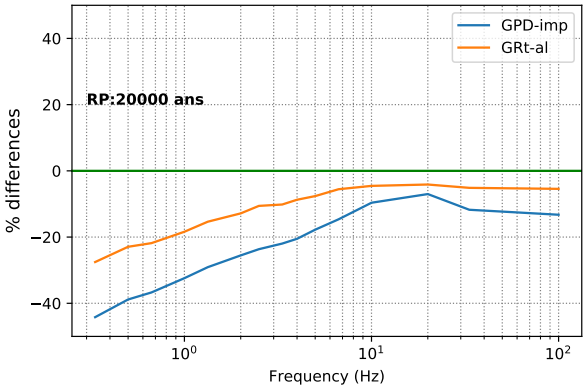

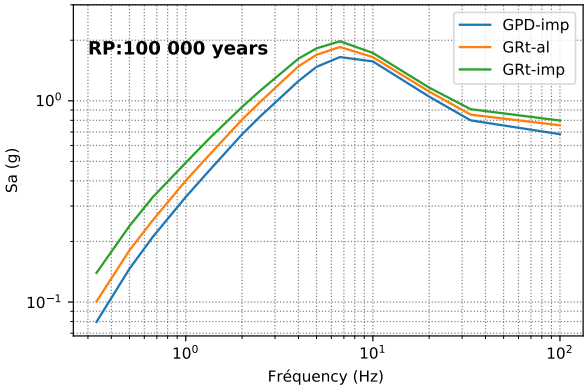

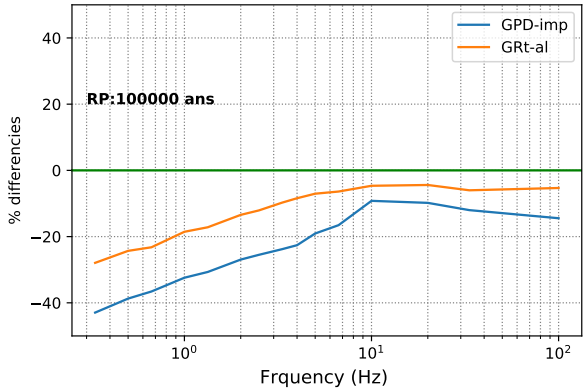

Fig. 19 Comparison of the Uniform Hazard Spectra (UHS) between the new recurrence models: Random Gutenberg-Richter *GRt-al*, Generalized Pareto Distribution *GPD-imp* and the common Gutenberg-Richter model *GRt-imp* for the return periods (RP): 475, 10 000, 20 000 and 100 000 years.

Fig. 20 Relative differences of the UHS calculated with the new recurrence models (*GPD-imp* and *GRt-al*) with respect to the common Gutenberg Richter model (*GRt-imp*) considered as a reference.

the PSHA calculation, which directly induces a reduction in the seismic hazard, precisely for low frequency component and for very long return periods (eg 100 000 years).

Impact of parameters uncertainty on the probabilistic seismic hazard In this section, we propagate the uncertainty on the estimation of the recurrence model parameters through PSHA calculations.
We generated 100 possible sets of parameters of each recurrence model, according to the asymptotic distribution of their estimators, which generated 400 branches in the PSHA logic-tree.
At each frequency and for each return period, we calculated the quantile of level 5%, 50% (median value) and 95%. Figure 21 shows the quantile curves of the UHS, for each recurrence model. To better understand the impact of the estimation uncertainty, we draw on Figure 22 the coefficient of variation of the sample values, at each frequency, defined as the ratio between the standard deviation and the mean of the values. The larger the coefficient of variation, the larger the variability around the mean value. The results show that from the frequency 5 Hz, *GRt-imp* has the largest coefficient of variation compared to *GPD-imp* and *GRt-al*: the uncertainty in the estimation of the truncated Gutenberg Richter model induces the greatest uncertainty on the hazard levels. In other words, calculations of hazard levels with the new recurrence models are more robust than those from the truncated Gutenberg Richter one with respect to the parameters estimation uncertainty. For lower frequencies, *GPD-imp* presents the greatest uncertainty with a peak at 30% at the frequency 0.33 Hz. One the other hand, at that frequency, *GRt-imp* and *GRt-al* have practically the same feature, largely below *GPD-imp*. This trend is the same for all return periods analysed in the present study.

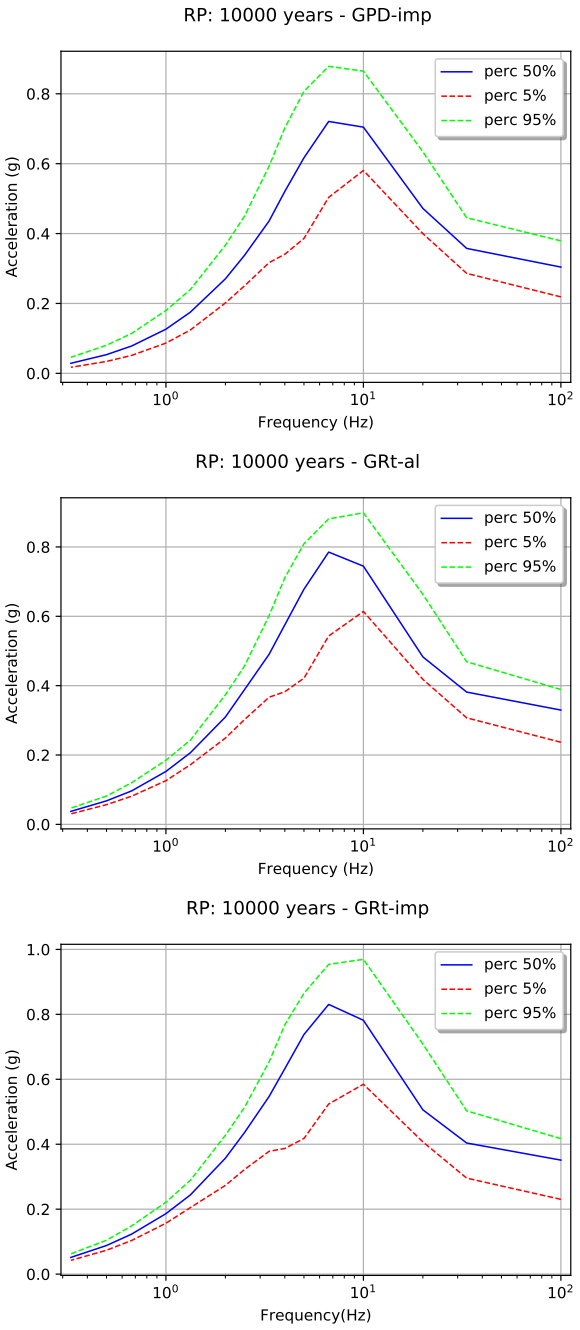

Fig. 21 5%, 50% and 95% quantile curves of the UHS calculated with the new recurrence models (*GPD-imp*, *GRt-al*) and the common Gutenberg-Richter model *GRt-imp*.

5 Conclusions

In this paper, we presented a new generation of earthquake recurrence models and we subsequently compared them to the truncated Gutenberg-Richter model that is commonly used in PSHA calculations. We evaluated their impact on probabilistic seismic hazard assessments, using the Alps data.

Both innovative models are based on an extreme value analysis, which avoids fixing a priori the maximum possible magnitude m_{max}. This value results from a statistical analysis adapted to extreme values. This feature is particularly interesting as there is no widely accepted method to estimate m_{max}.

The Random Gutenberg-Richter model is a mix of the truncated Gutenberg-Richter model and the GPD-based model. It looks promising because:

– the Exponential distribution that has been widely accepted by the seismologist community, is still used to model the magnitudes distribution,

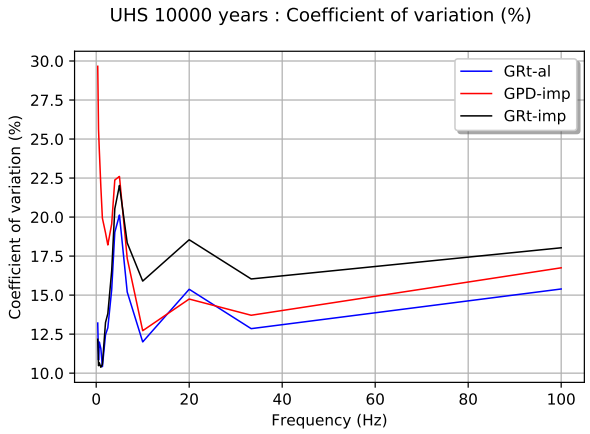

Fig. 22 Uncertainties on parameters estimation: coefficient of variation of the UHS calculated with the recurrence models *GPD-imp*, *GRt-al* and the common Gutenberg-Richter model *GRt-imp*.

– the randomness of M_{max} allows to take into account the uncertainty on the maximum possible magnitude value, whose determination is a tricky matter,
– the distribution of M_{max} relies on an extreme value analysis that aims at modeling the behavior of the extreme magnitudes.

This new generation of recurrence models introduce a reduction of the hazard compared to the truncated Gutenberg-Richter model commonly used in PSHA. This decrease is significant for all frequencies below 10 Hz, above all for very long return periods (e.g. 100,000y). It is estimated between 10% and 50% depending on the frequency. These new recurrence models are expected to result in a more realistic assessment of the probabilistic seismic hazard.

6 Declarations

Not applicable.

References

1. URL www.sisfrance.fr.
2. Abrahamson, N.: State of the practice of seismic hazard evaluation. Proc GeoEng, Melbourne, Australia (2000)
3. Abrahamson, N., Birkhauser, P., Koller, M., Mayer-Rosa, D., Smit, P., Sprecher, C., Tinic, S., Graf, R.: A comprehensive probabilistic seismic hazard assessment for nuclear power plant in switzerland. Proc 12th Eur Conf Earthquake Eng, London, UK, paper 633 (2002)
4. Abrahamson, N., Silva, W., Kamai, R.: Summary of the ask14 ground-motion relation for active crustal regions. Earthquake Spectra **30**(3), 1025–1055 (2014)
5. Akkar, S., Bommer, J.: Empirical equations for the prediction of pga, pgv and spectral accelerations in europe, the mediterranean region and the middle east. Seismol Res Lett **81**(2), 195–206 (2010)
6. Anderson, J., Wesnousky, G., Stirling, M.: Earthquake size as a function of slip rate. Bull Seism Soc Am **86**, 683–690 (1996)
7. Baudin, M., Dutfoy, A., Popelin, A., Iooss, B.: OpenTURNS: An Industrial Software for Uncertainty Quantification in Simulation. Handbook of Uncertainty Quantification, Springer (2017). URL www.openturns.org
8. Berge-Thierry, C., Voldoire, F., Ragueneau, F., Lopez-Caballero, F., LeMaoult, A.: Main achieve-ments of the multidisciplinary sinaps@ research project: Towards an integrated approach to per-form seismic safety analysis of nuclear facilities. Pure Appl Geophys **177**, 2299–2351 (2020)
9. Bindiand, D., Massa, M., Luzi, L., Ameri, G., Pacor, F., Puglia, R., Augliera, P.: Pan-european ground-motion prediction equations for the average horizontal component of pga, pgv, and 5%-damped psa at spectral periods up to 3.0 s using the resorce dataset. Bull Earthquake Eng **12**(1), 391–430 (2014)
10. Cara, M., Cansi, Y., Schlupp, A., Arroucau, P.: Sihex: a new catalog of instrumental seismicity for metropolitan france. Bull Soc Geol Fr **186**, 3–19 (2015)
11. Cara, M., Denieul, M., Sèbe, O., Delouis, B., Cansial, Y., Schlupp, A.: Magnitude mw in metropolitan france. Journal of Seismology **21**, 551–565 (2017)
12. Cauzzi, C., Faccioli, E., E., V.M., Bianchini, A.: Updated predictive equations for broadband (0.01 to 10 s) horizontal response spectra and peak ground motions, based on a global dataset of digital accelerationrecords. Bull Earthquake Eng **13**, 1587–1612 (2015)
13. Cornell, A.: Engineering seismic risk analyses. Bull Seism Soc Am **58**(5), 1583–1606 (1968)
14. Cosentino, P., Ficara, V., Luzio, D.: Truncated exponential frequency-magnitude relationship in earthquakes statistics. Bull Seism Soc Am **67**, 1615–1623 (1977)
15. Drouet, S., Ameri, G., Dortzand, K.L., Secanell, R., Senfaute, G.: Probabilistic seismic hazard map for the metropolitan france. Bull Earthquake Eng **18** (2020)
16. Dutfoy, A.: Estimation of tail distribution of the annual maximum earthquake magnitude using extreme value theory. Pure Appl Geophys **170**(9-10), 1361–1372 (2018)
17. Dutfoy, A.: Earthquake recurrence model based on an extreme value distribution for unequal observation periods and imprecise magnitudes. Pure Appl Geophys (accepted) (2020)
18. Dutfoy, A.: Estimation of the gutenberg-richter earthquake recurrence parameters for unequal observation periods and imprecise magnitudes. Pure Appl Geophys **177**(10), 4597–4606 (2020)
19. Grünthal, G., Stromeyer, D., Bosse, C., Cotton, F., Bindi, D.: The probabilistic seismic hazard assessment of germany-version 2016, considering the range of epistemic uncertainties and aleatory. Bull Earthquake Eng **16**, 4339–4395 (2018)
20. Gutenberg, B., Richter, C.: Magnitude and energy of earthquakes. Science **83**, 183–185 (1936)
21. Gutenberg, B., Richter, C.: Earthquakes magnitude, intensity, energy and acceleration. Bull Seism Soc Am **46**(3), 105–145 (1945)
22. Kijko, A.: Estimation of the maximum earthquake magnitude mmax. Pure Appl Geophys **161**, 1655–1681 (2004)
23. Kijko, A.: On bayesian procedure for maximum earthquake magnitude estimation. Res in Geophys **2**(e7) (2012)
24. Kijko, A., Graham, G.: Parametric-historic procedure for probabilistic seismic hazard analysis. part 1. estimation of the maximum regional earthquake magnitude mmax. Pure Appl Geophys **151**, 413–442 (1998)

25. Manchuel, K., Traversa, P., Baumont, D., Cara, M., Nayman, E., Durouchoux, C.: The french seismic catalogue (fcat-17). Bull Earthquake Eng **16**(10), 2227–2251 (2018)
26. McCalpin, J.: Paleoseimology. Academic Press, New-York (1996)
27. Pagani, M., Monelli, D., G.Weatherill: Openquake engine: an open hazard (and risk) software for the global earthquake model. Seismol. Res. Lett. **85**(3), 692–702 (2014)
28. Page, R.: Aftershock and microaftershocks. Bull.Seism. Soc. Am. **58**, 1131–1168 (1968)
29. Pecker, A., Faccioli, E., Gurpinar, A., Martin, C., Renault, P.: An overview of the SIGMA research project. Springer, Berlin (2017)
30. Pickands, J.: Statistical inference using extreme order statistics. Annals of Statistics **3**, 119–131 (1975)
31. Pisarenko, V., Sornette, A., Sornett, D., Rodkin, M.: Characterization of the tail of the distribution of earthquake magnitudes by combining the gev and gpd description of extreme value theory. Pure Appl Geophys **171**, 1599–1624 (2014)
32. Renault, P.: Bollettino di Geofisica Teorica ed Applicata **55**(1), 149–164 (2014)
33. Senfaute, G., Pecker, A., Labbé, P., Sidaner, J., Berge-Thierry, C., Rzepka, J., Contri, P.: Contribution of the sigma research program to analyses of uncertainties in seismic hazard assessment. 9ième Colloque National. AFPS, France (2015)
34. Traversa, P., Manchuel, K., Mayor, J.: On the use of cross-border macroseismic data to improve the estimation of past earthquakes seismological parameters. 2ECEES conference, Istanbul, Turkey. **12** (2014)
35. Turcotte, D.: Seismicity and self-organized criticality. Phys Earth Plan In **111**, 275–293 (1999)
36. Wells, D.L., Coppersmith, K.J.: New empirical relationships among magnitude, rupture length, rupture width, rupture area, and surface displacement. Bull.Seism. Soc. Am. **84**, 974–1002 (1994)
37. Wheeler, R.L.: Methods of Mmax Estimation East of Rocky Mountains. U.S. Geological Survey, Open-File Report 2009-1018 (http/pubs.ugs.gov/of/2009/1018/pdf/OF09-1018.pdf). Accessed February 2013 (2009)

Figures

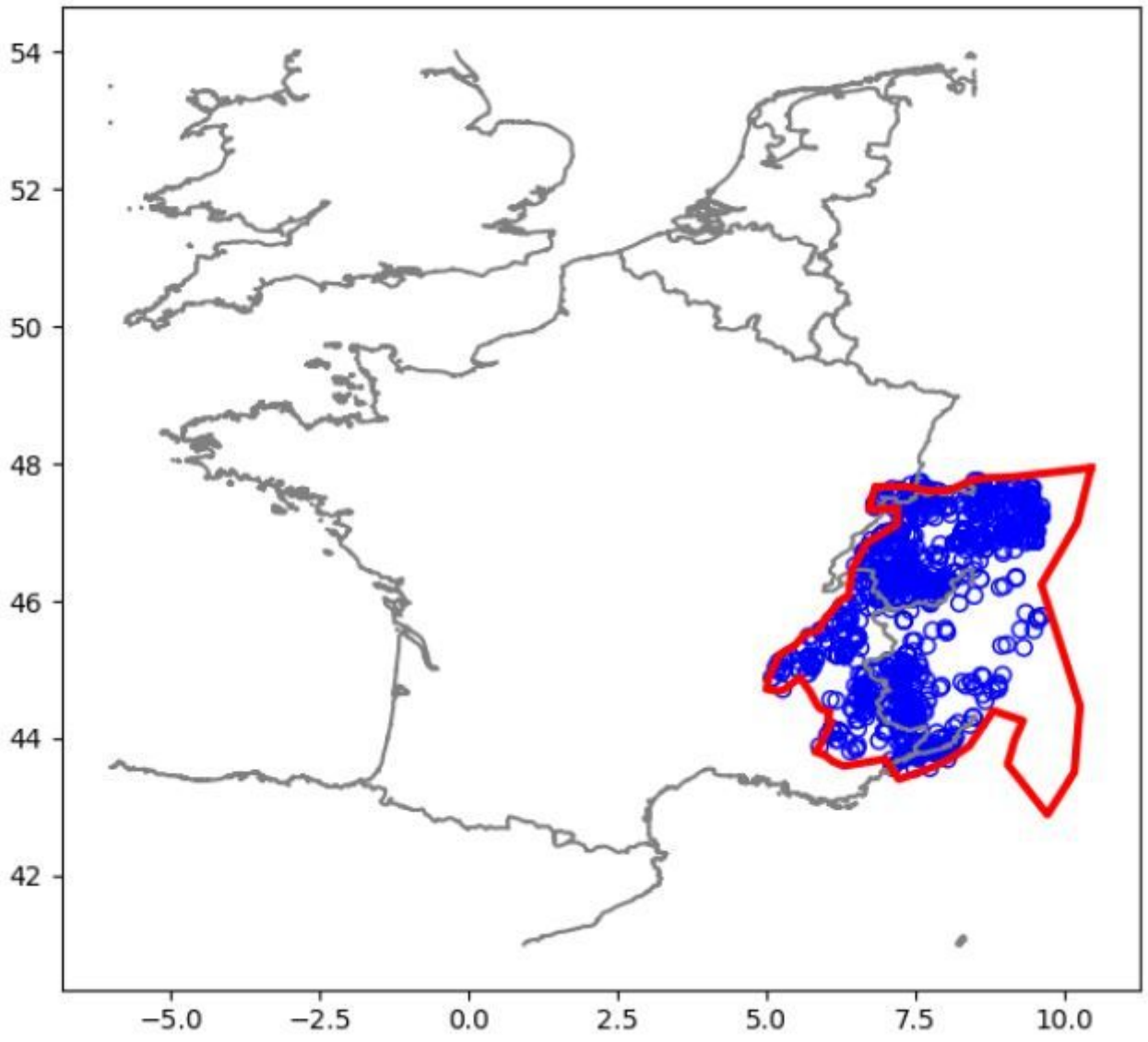

Figure 1

Earthquakes in the Alps in France (longitude - latitude units). Note: The designations employed and the presentation of the material on this map do not imply the expression of any opinion whatsoever on the part of Research Square concerning the legal status of any country, territory, city or area or of its authorities, or concerning the delimitation of its frontiers or boundaries. This map has been provided by the authors.

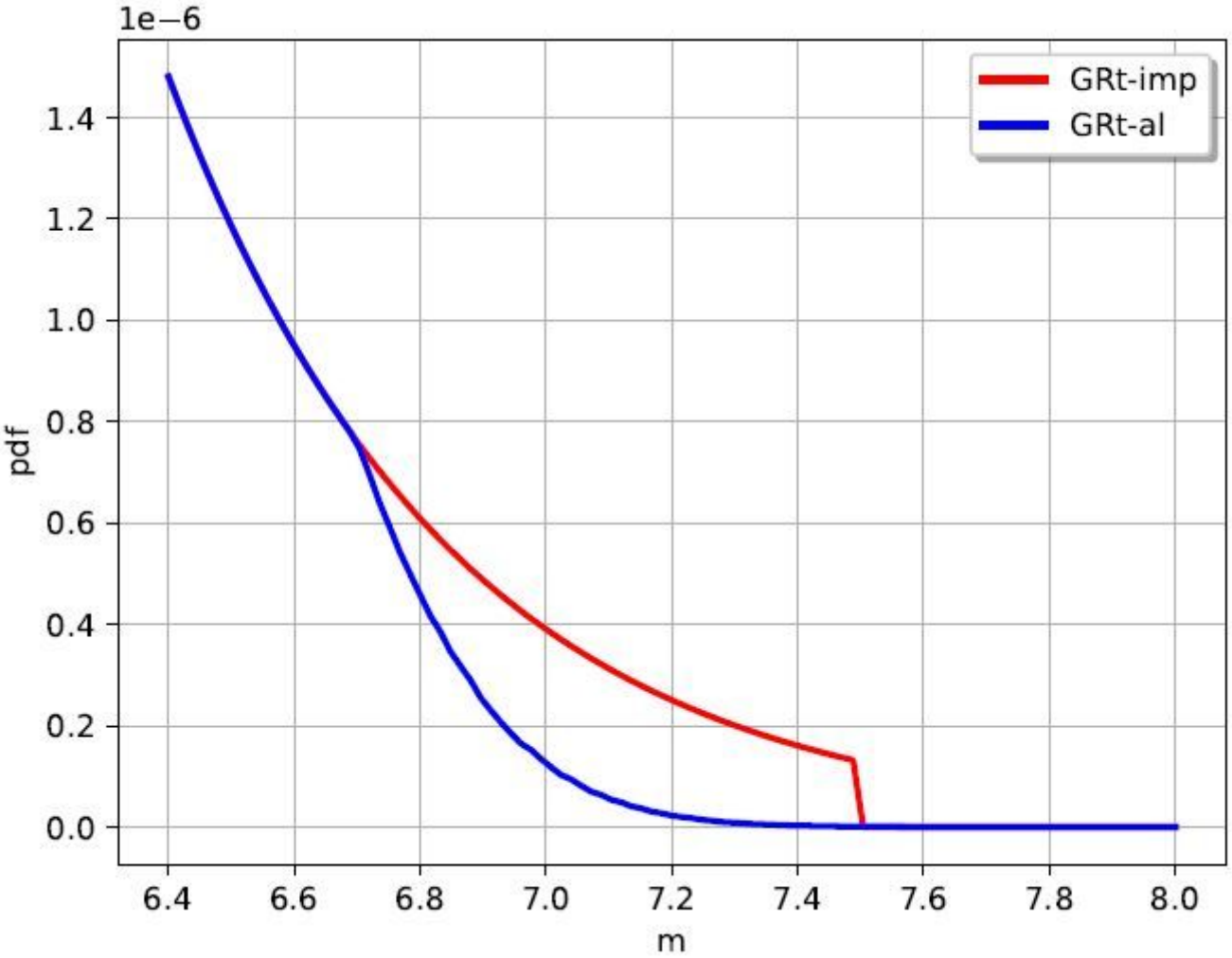

Figure 2

Distribution of magnitudes: Exponential(^b log 10) truncated to mmax = 7:5Mw (GRt-imp) or to the random variable Mmax ~ N(μ = 6:75Mw; σ2 = 7:63 10-2) truncated to [6:69Mw;+1[(GRt-al).

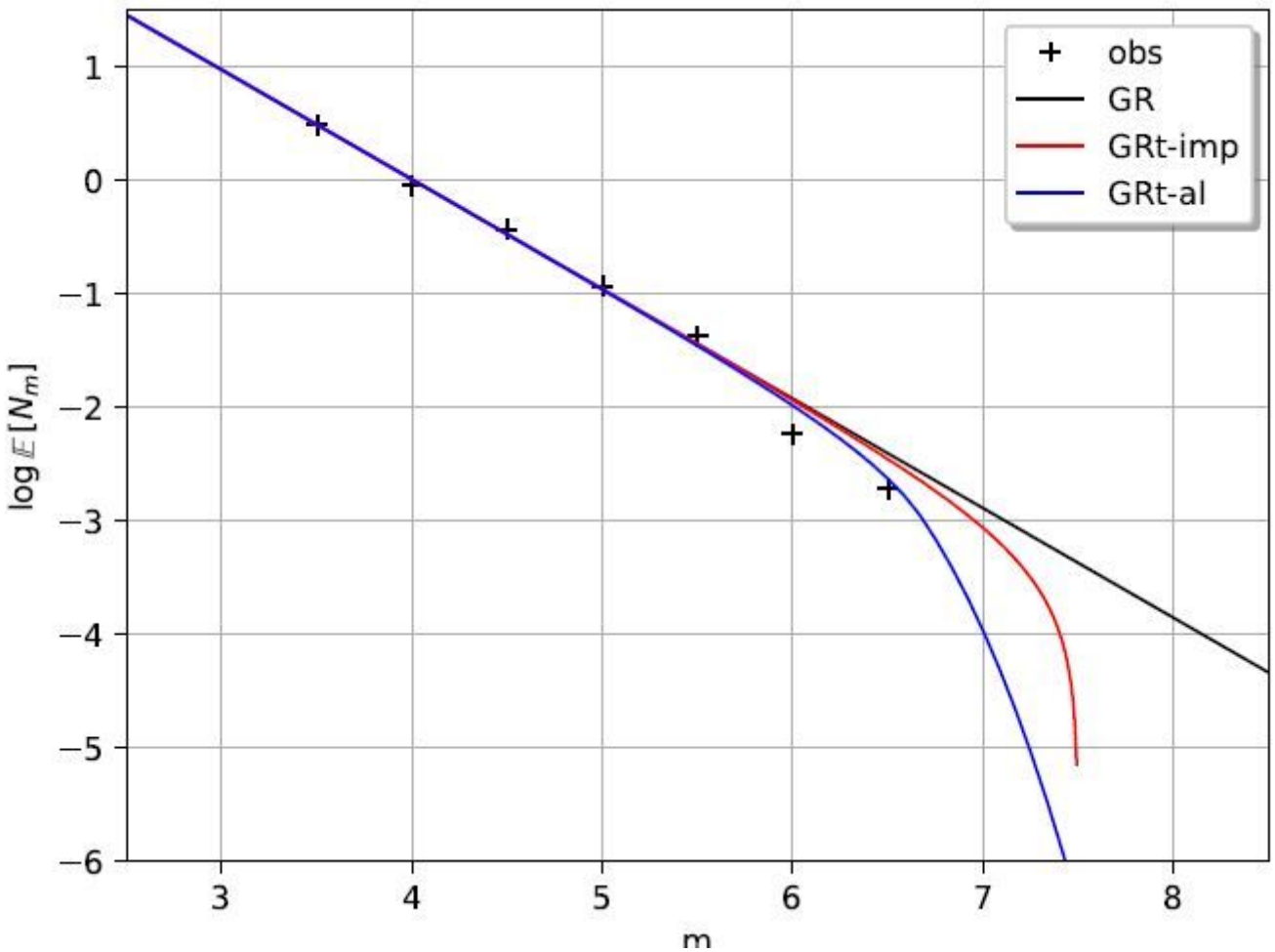

Figure 3

Recurrence model associated to the Exponential(^b log 10) truncated to mmax = 7:5Mw (GRt-imp); or to the random variable Mmax ~ N(6:75Mw; 7:63 10-2) truncated to [6:69Mw;+1[(GRt- al).

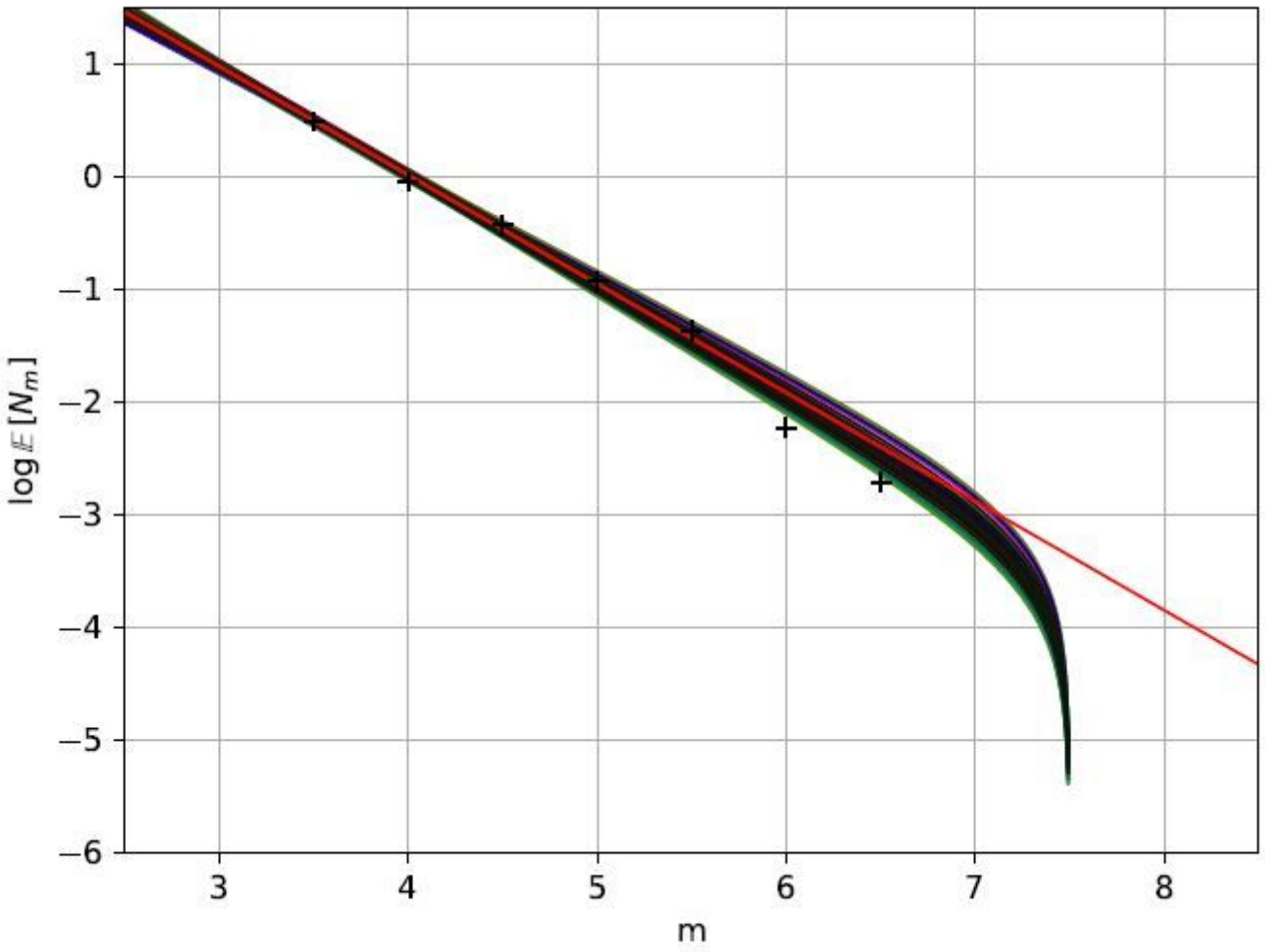

Figure 4

GRt-imp: Uncertainties on (^b; ^a): 100 possible recurrence models.

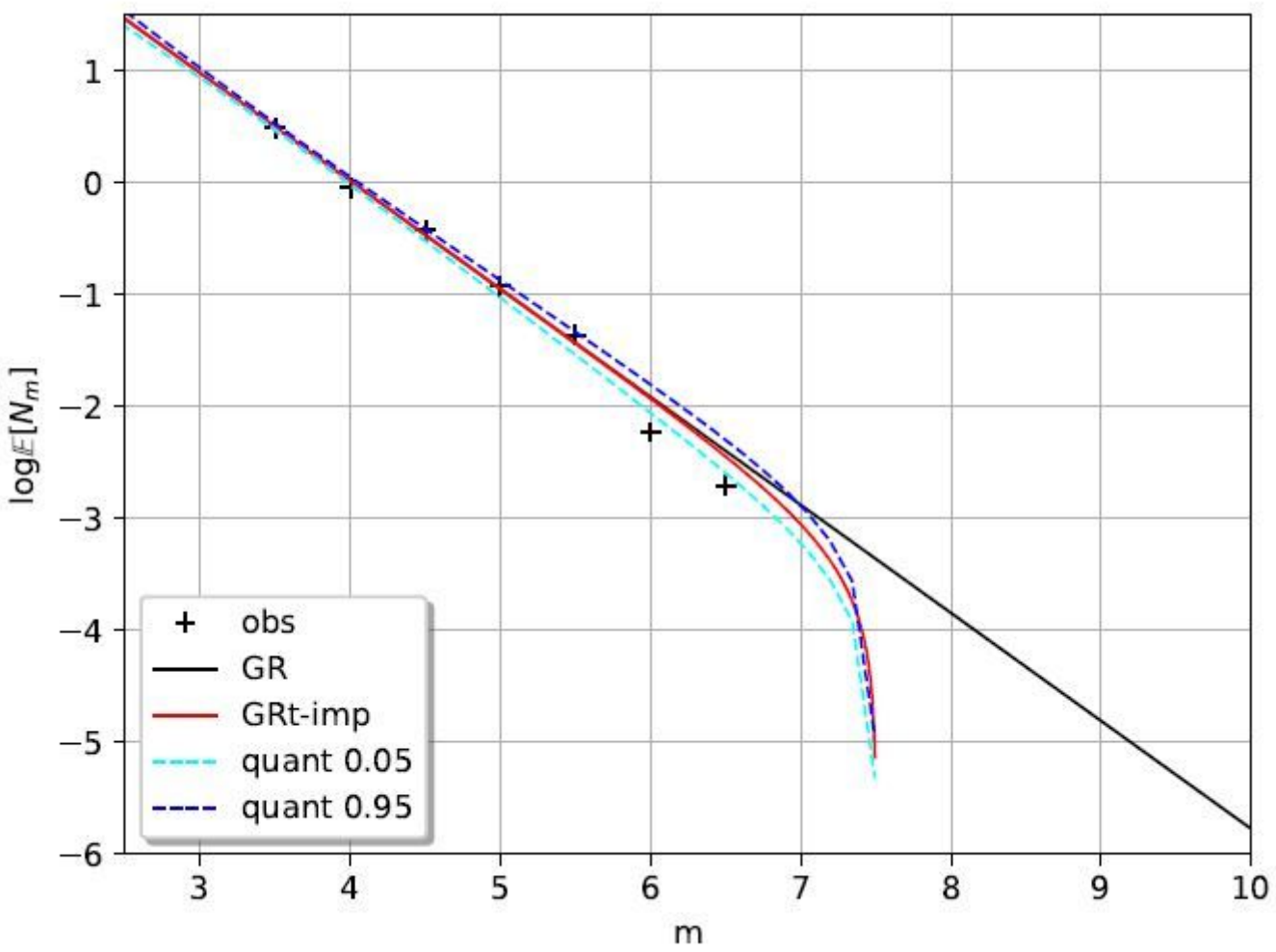

Figure 5

GRt-imp: uncertainties on the recurrence model due to uncertainties on (^b; ^a): quantile curves of level 5% and 95%, built from 106 models.

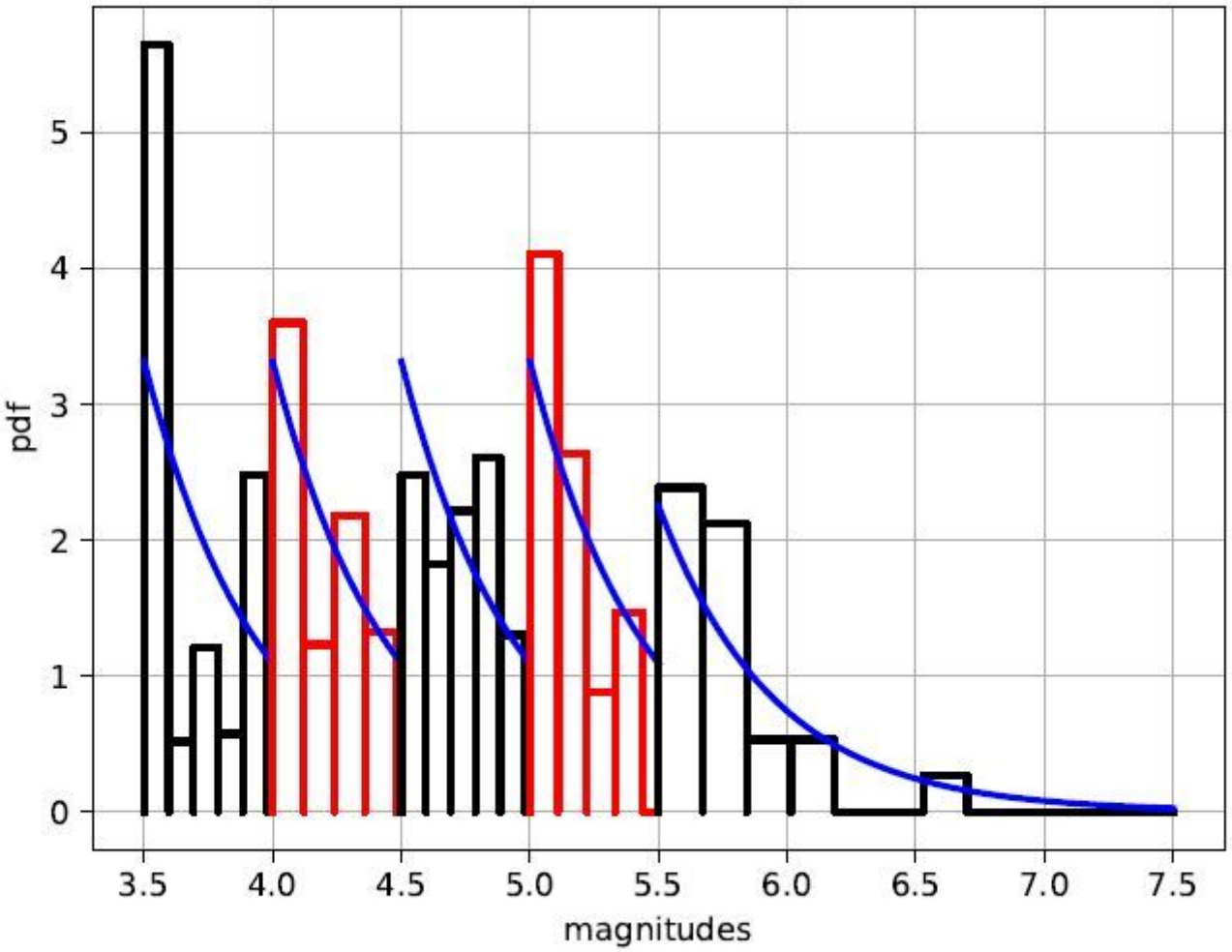

Figure 6

GRt-imp: Validation of the magnitudes distribution: empirical and estimated distributions of MjM 2 Ck for each class Ck.

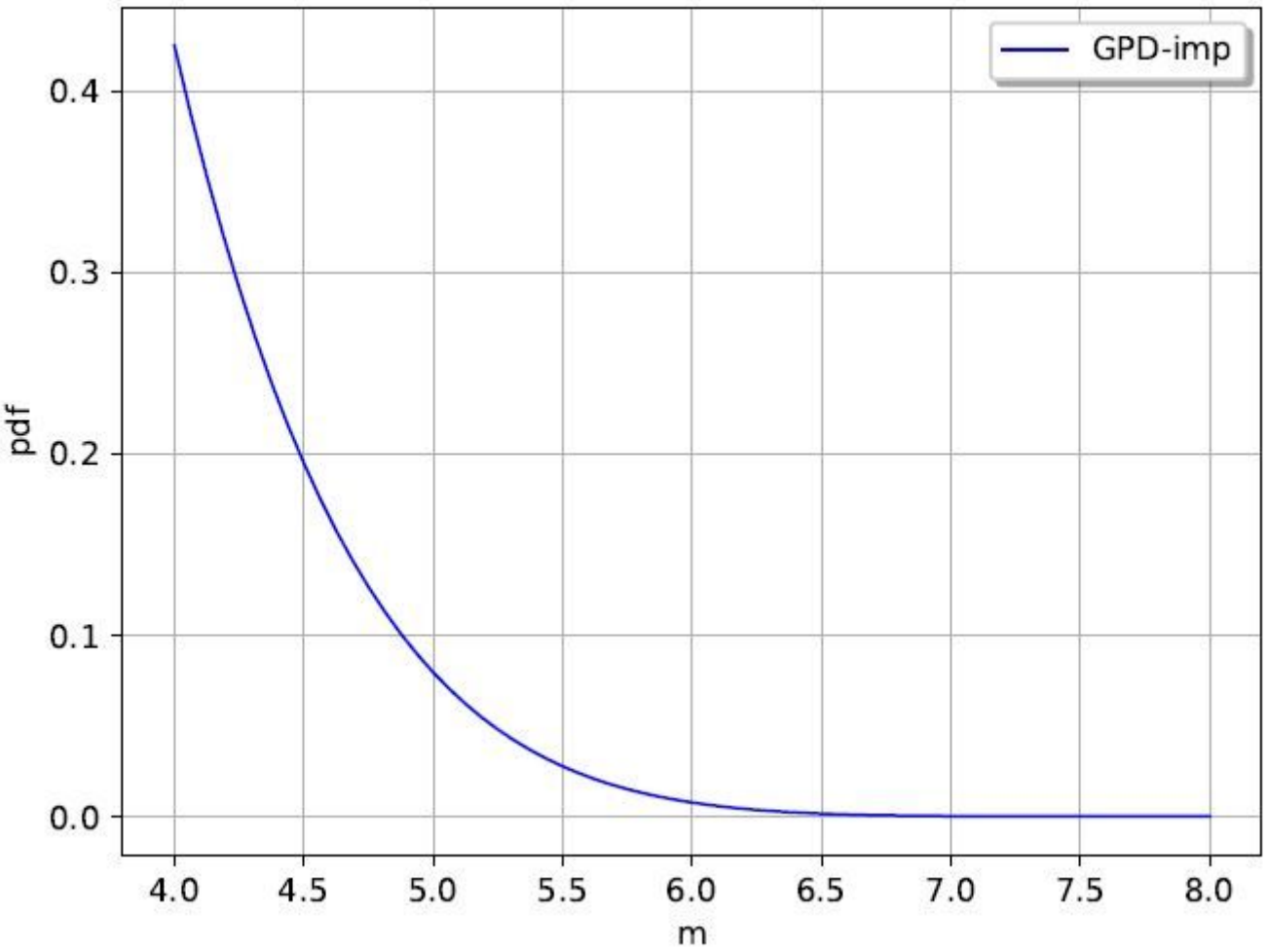

Figure 7

GPD-imp: Tail distribution of magnitudes M0 = MjM ≥ m0 based on the Generalized Pareto Distribution GPD(^σ; ^ξ) for magnitudes larger than u = 4:0Mw.

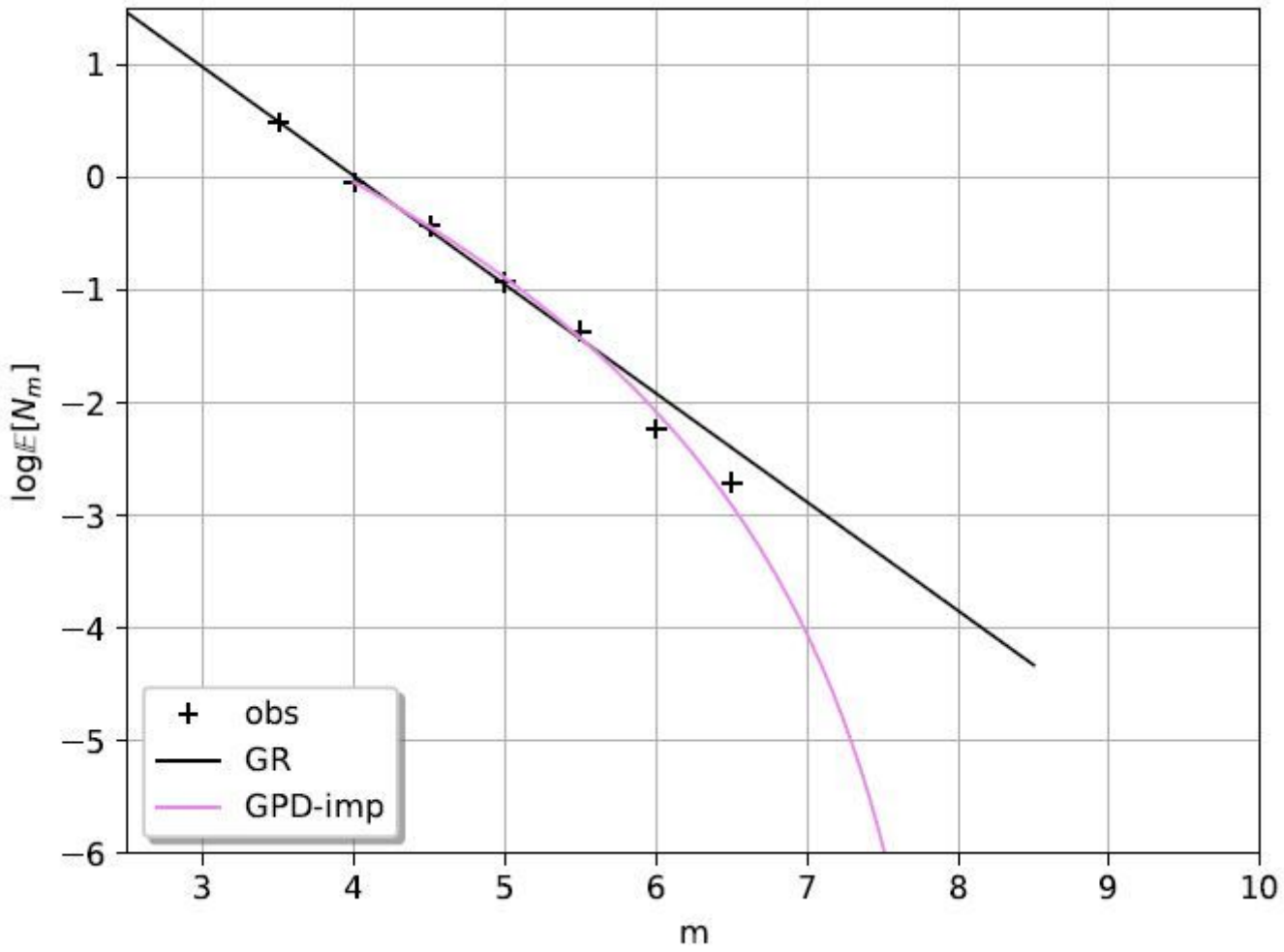

Figure 8

GPD-imp: Recurrence model associated to the GPD(^σ; ^ξ) tail distribution for magnitudes larger than u = 4:0Mw and the P(^μu) counting distribution.

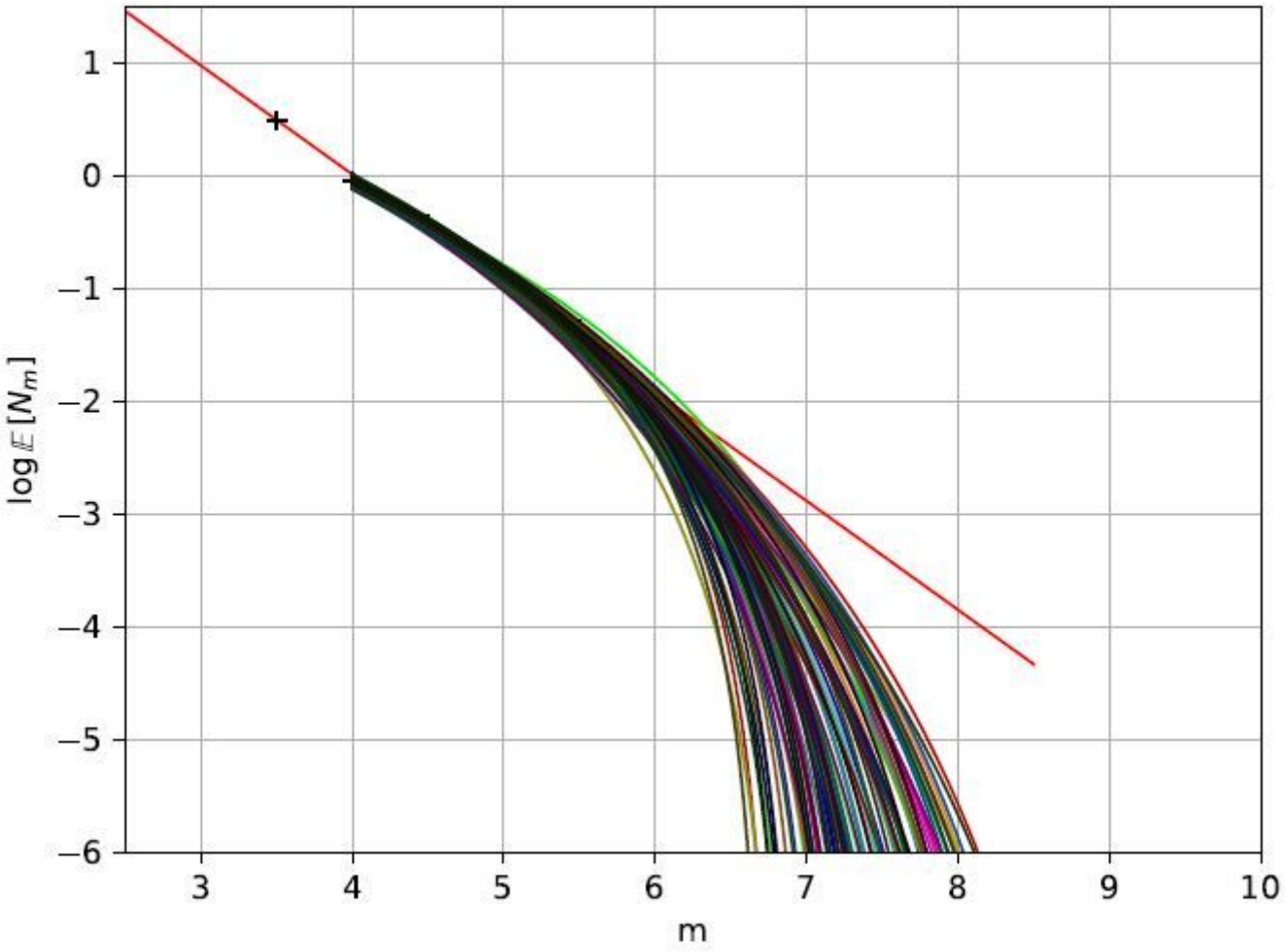

Figure 9

GPD-imp: Uncertainties on (^σ, ^ξ; ^μu): 100 possible recurrence models.

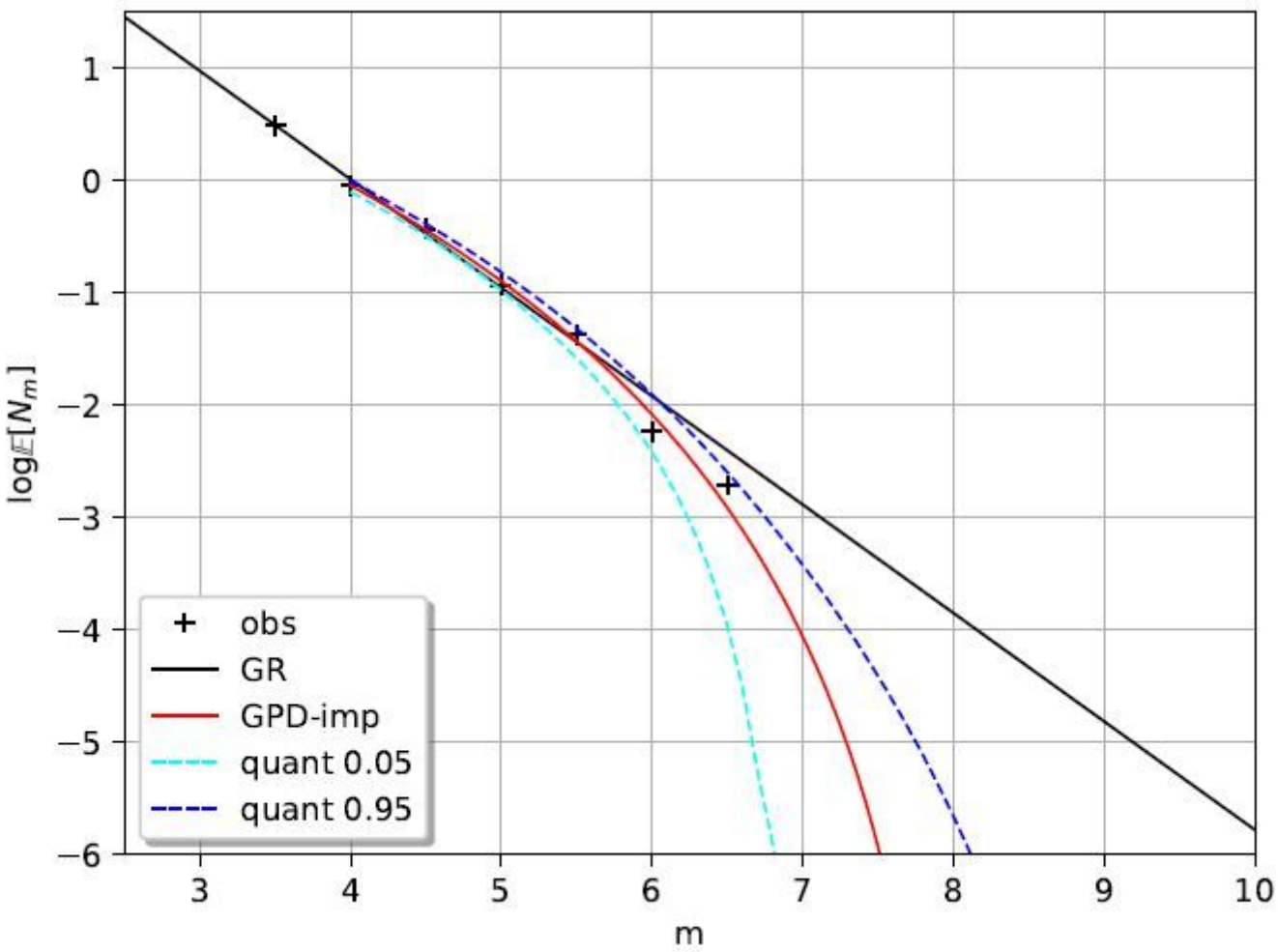

Figure 10

GPD-imp: Uncertainties on the recurrence model due to uncertaintes on (^σ, ^ξ; ^μu): quantile curves of level 5% and 95%, built from 106 models.

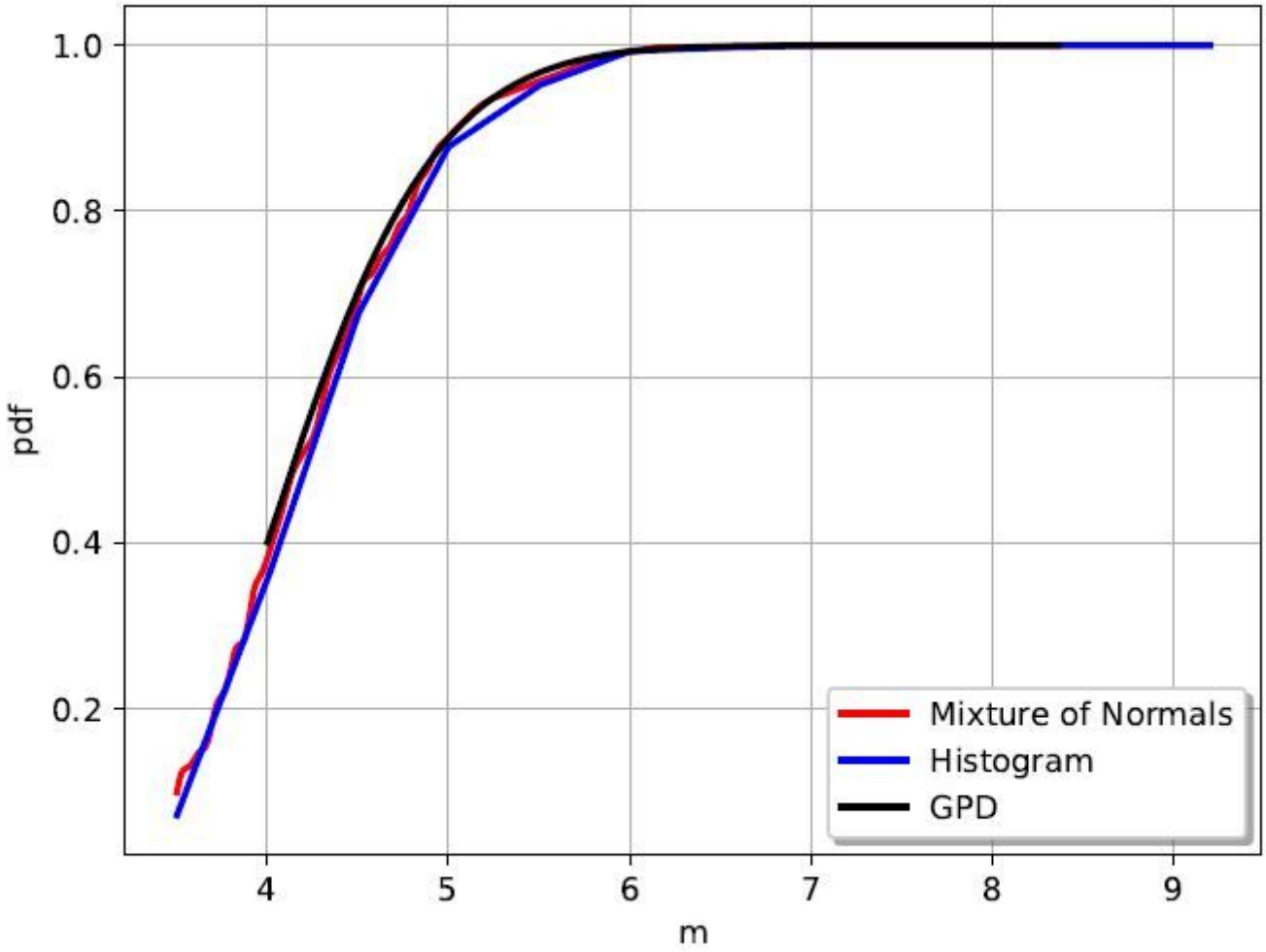

Figure 11

GPD-imp: Validation of the annual maximum magnitudes distribution.

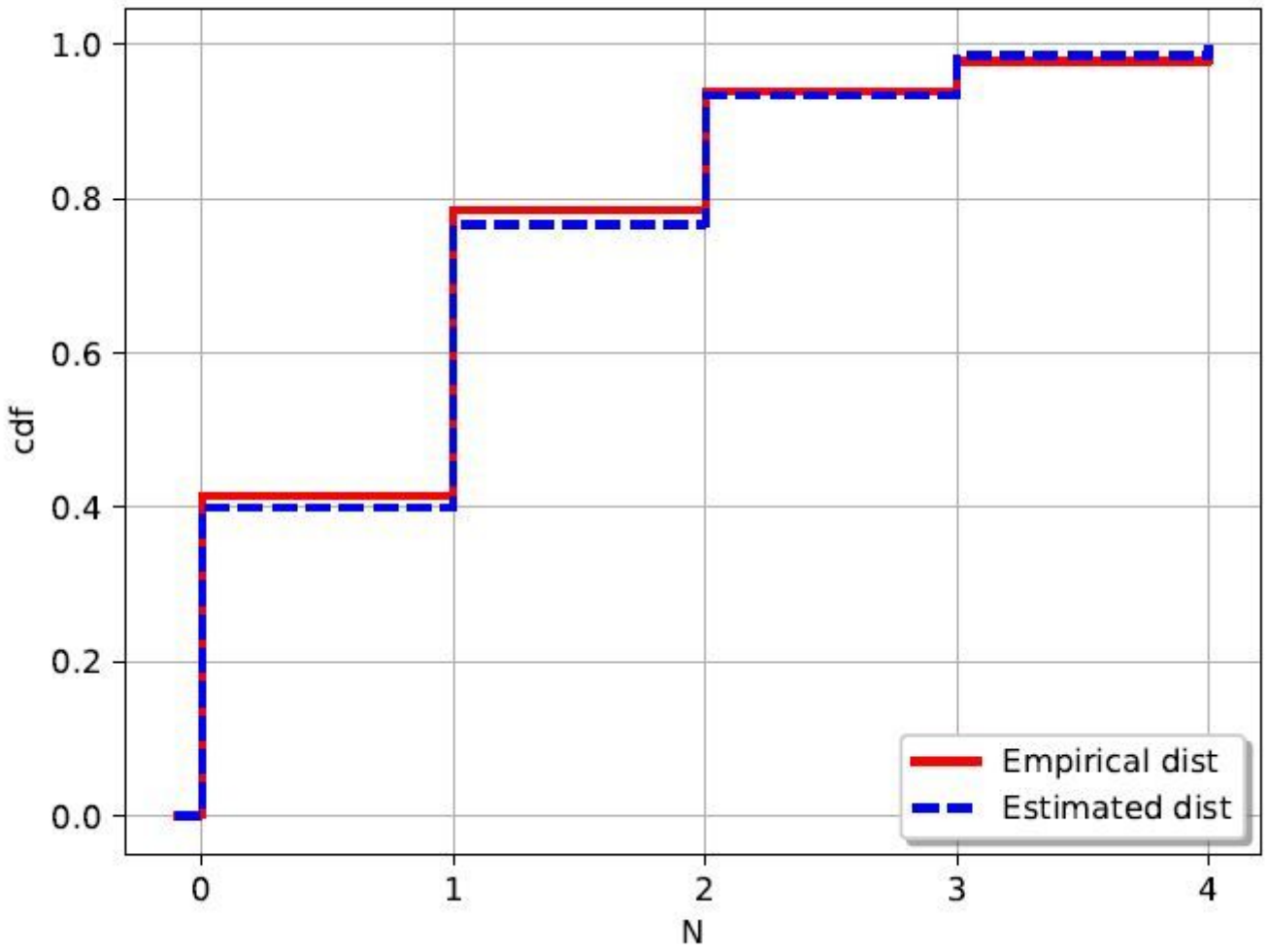

Figure 12

GPD-imp: Validation of the annual counting distribution of earthquakes with magnitudes larger than u = 4:0Mw.

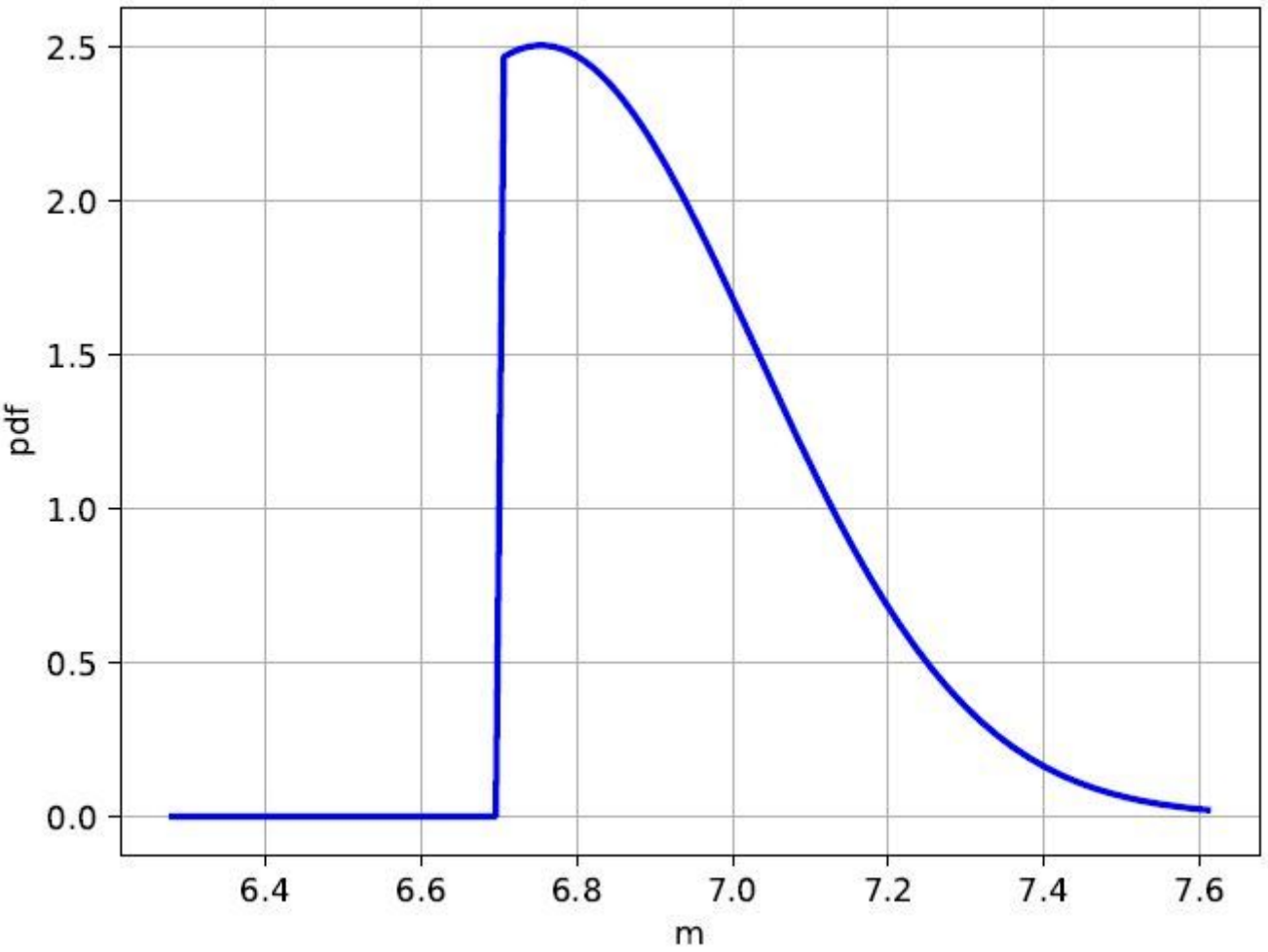

Figure 13

GRt-al : Distribution of the random upper bound Mmax of the Exponential distribution of magnitudes.

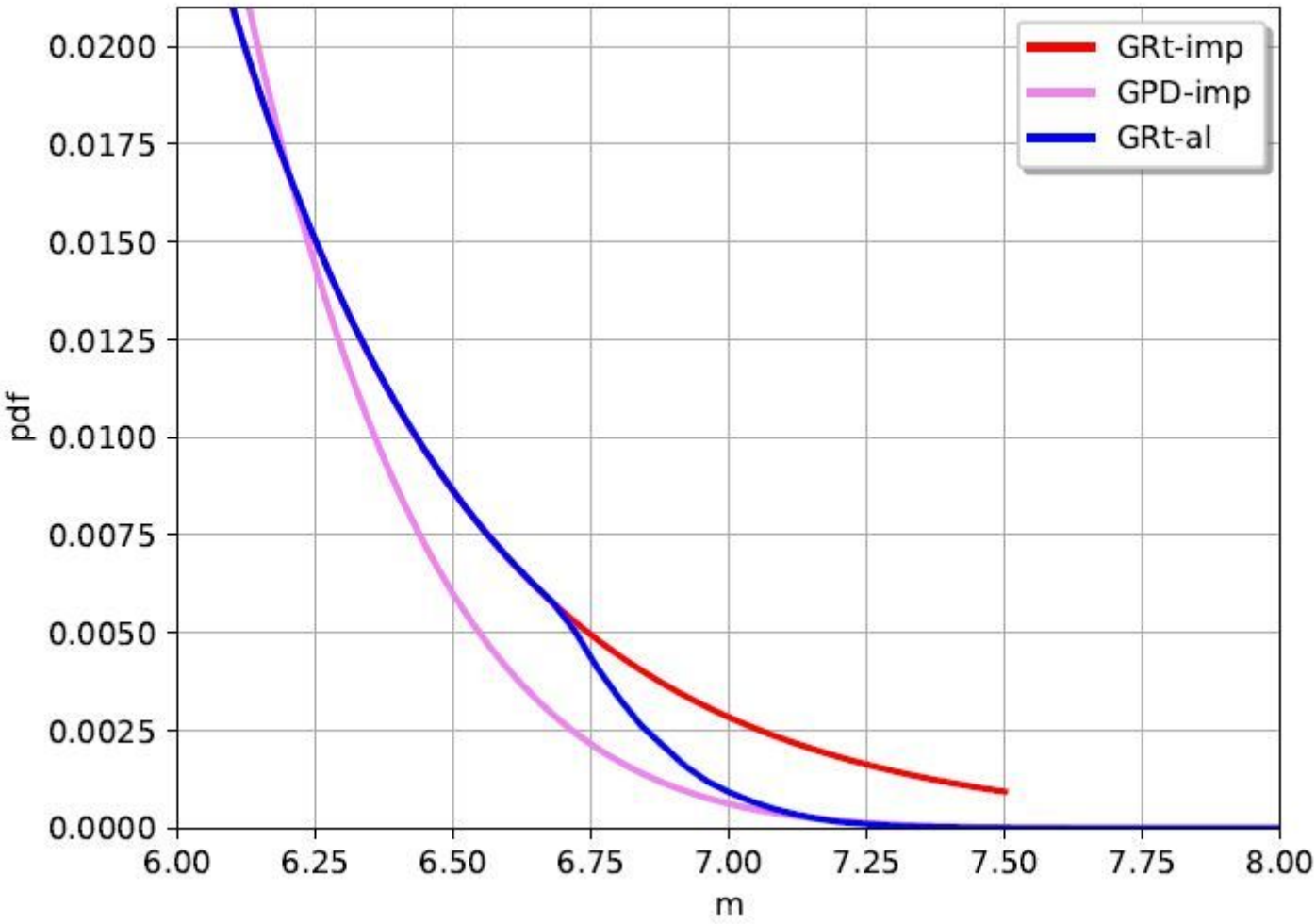

Figure 14

Distribution of Mu = MjM ≥ u based on the Exponential distribution truncated to mmax = 7:5Mw (GRt-imp), on the Exponential distribution truncated to the random magnitude Mmax (GRt-al) or based on the extreme value distribution GPD (GPD-imp): zoom on magnitudes larger than 6:0Mw.

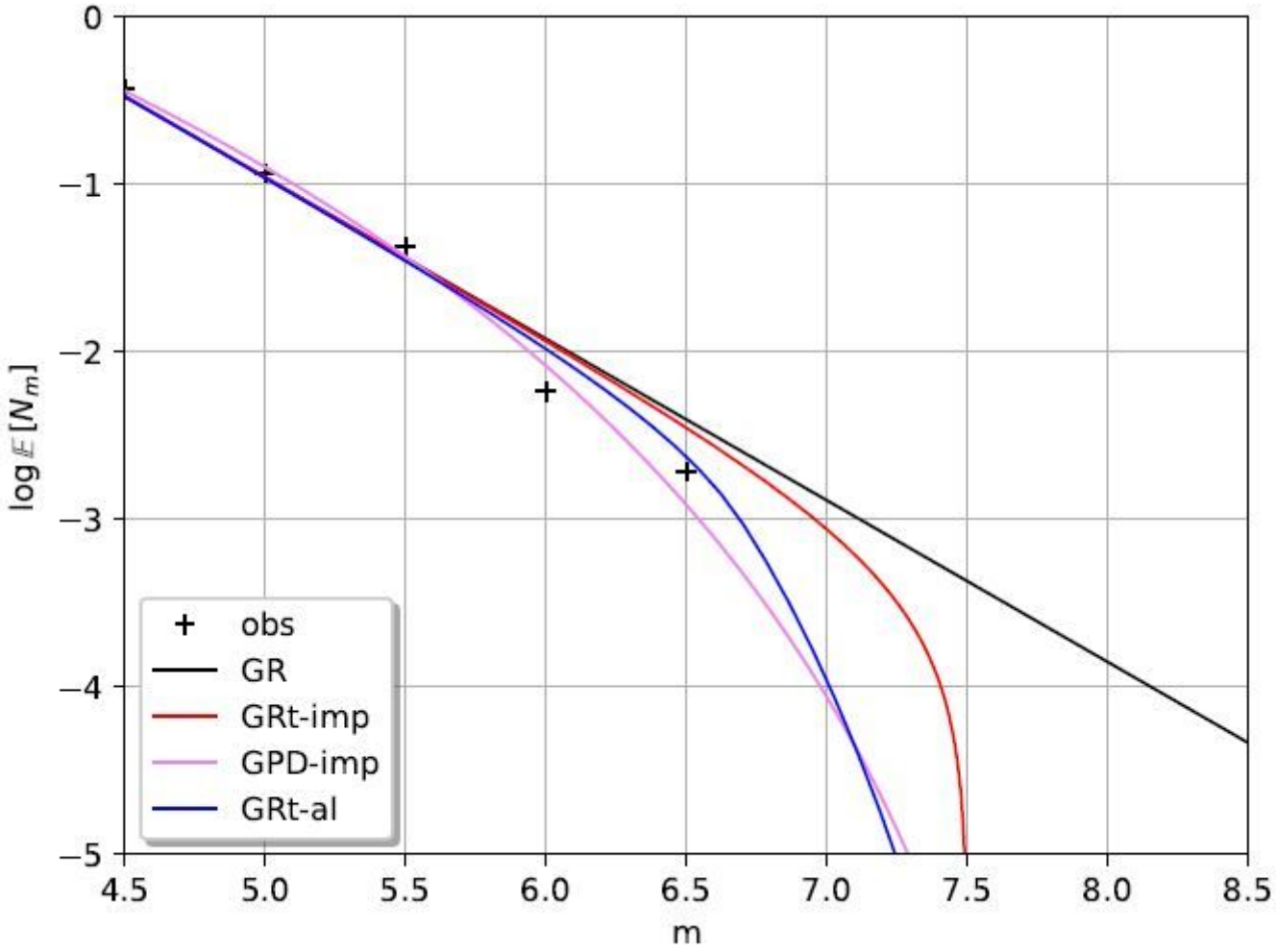

Figure 15

Recurrence models based on the Exponential distribution truncated to mmax = 7:5Mw (GRt-imp), on the Exponential distribution truncated to the random magnitude Mmax (GRt-al) or based on the extreme value distribution GPD (GPD-imp), compared to the Gutenberg-Richter straight line.

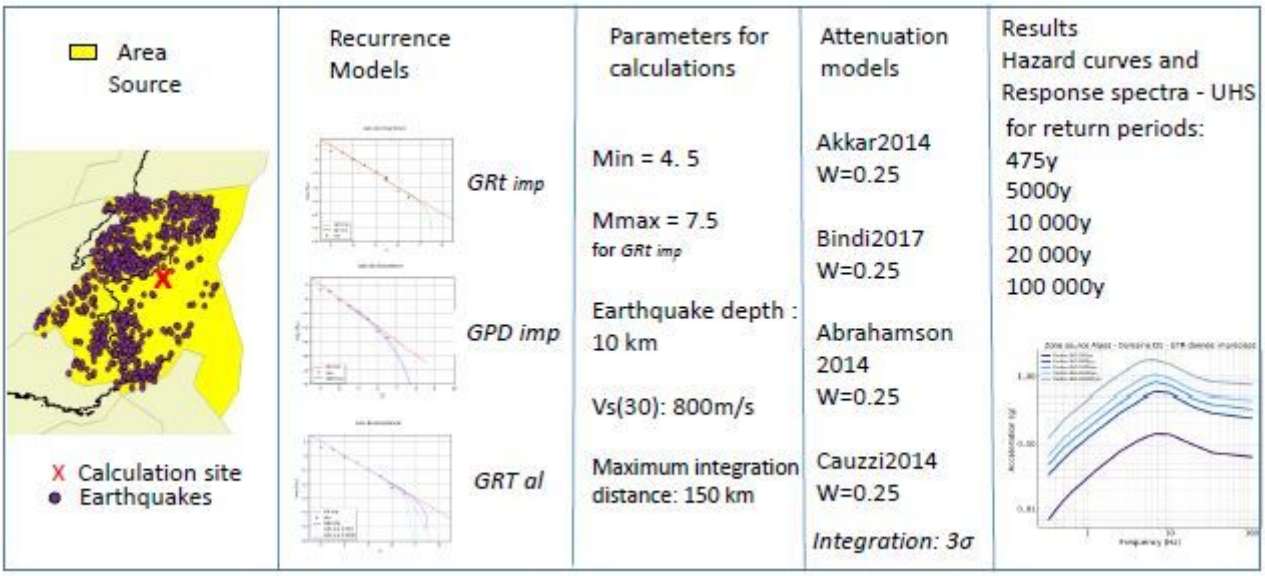

Figure 16

PSHA structure recurrence models (truncated Gutenberg Richter model (GRt-imp), Generalized Pareto Distribution model (GPD-imp) and Random Gutenberg Richter model (GRt-al)); in yellow the area source denition, in red the site for seismic hazard evaluation; parameters for calculation and attenuation models selected.

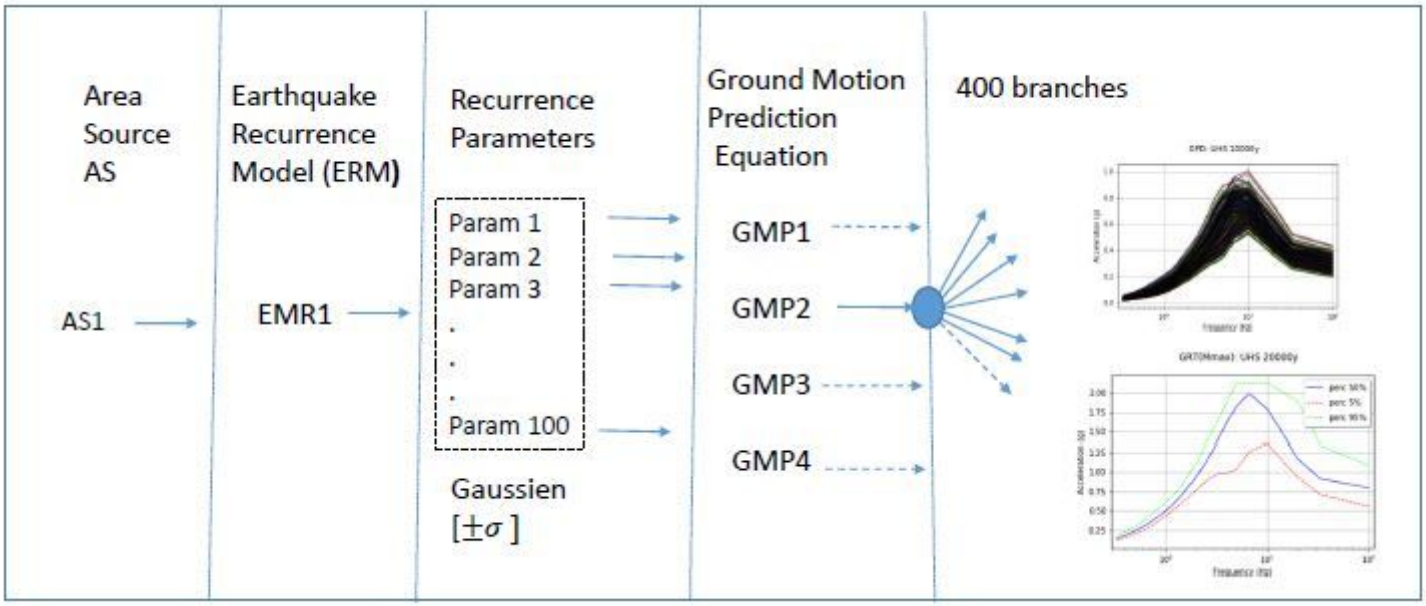

Figure 17

Logic-tree used to perform PSHA calculations, the model is made of 400 branches.

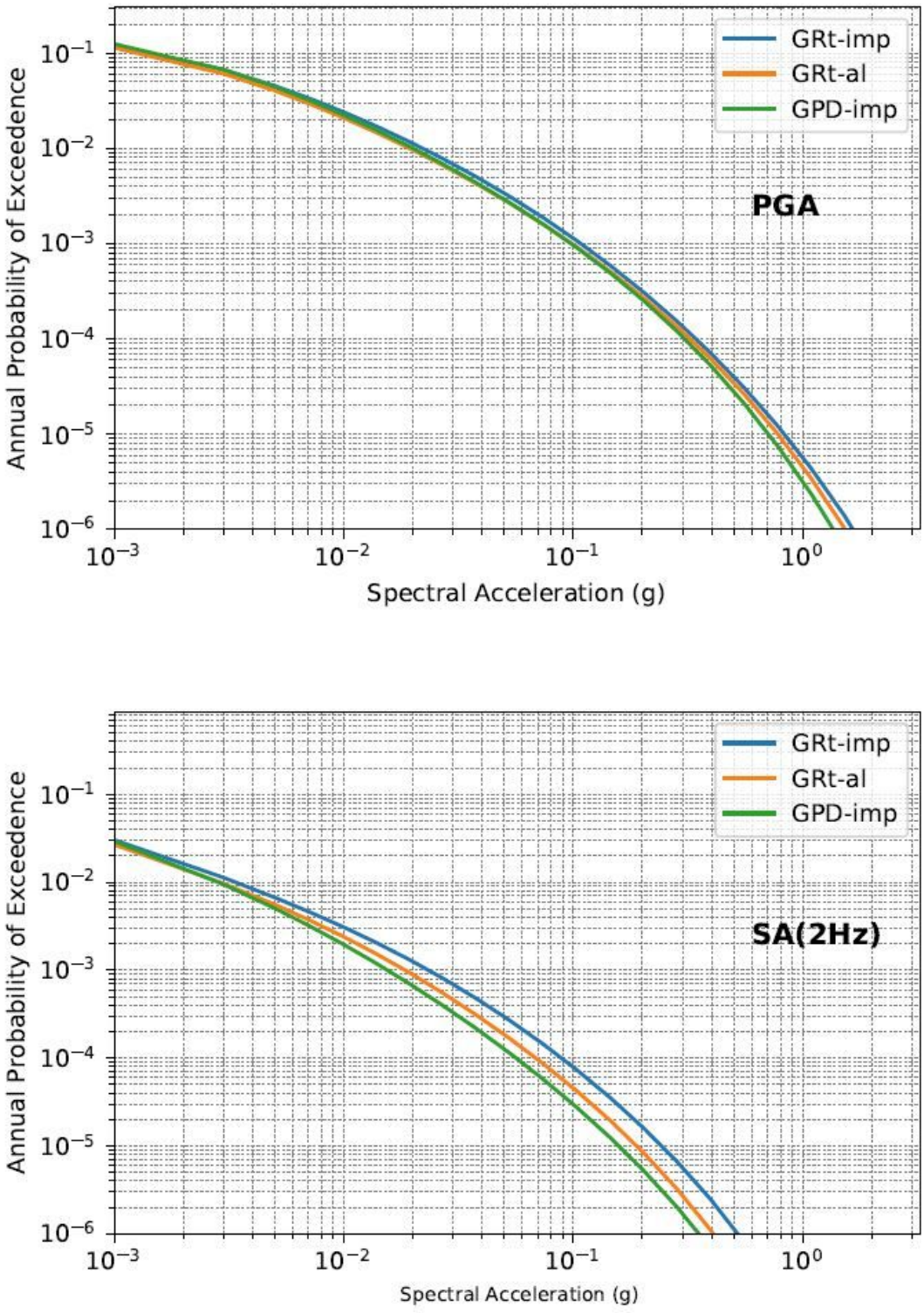

Figure 18

Comparison of the seismic hazard curves between the new recurrence models: Random Gutenberg-Richter GRt- al, Generalized Pareto Distribution GPD-imp, and the common Gutenberg Richter model GRt-imp, for spectral accelerations PGA and 2 Hz.

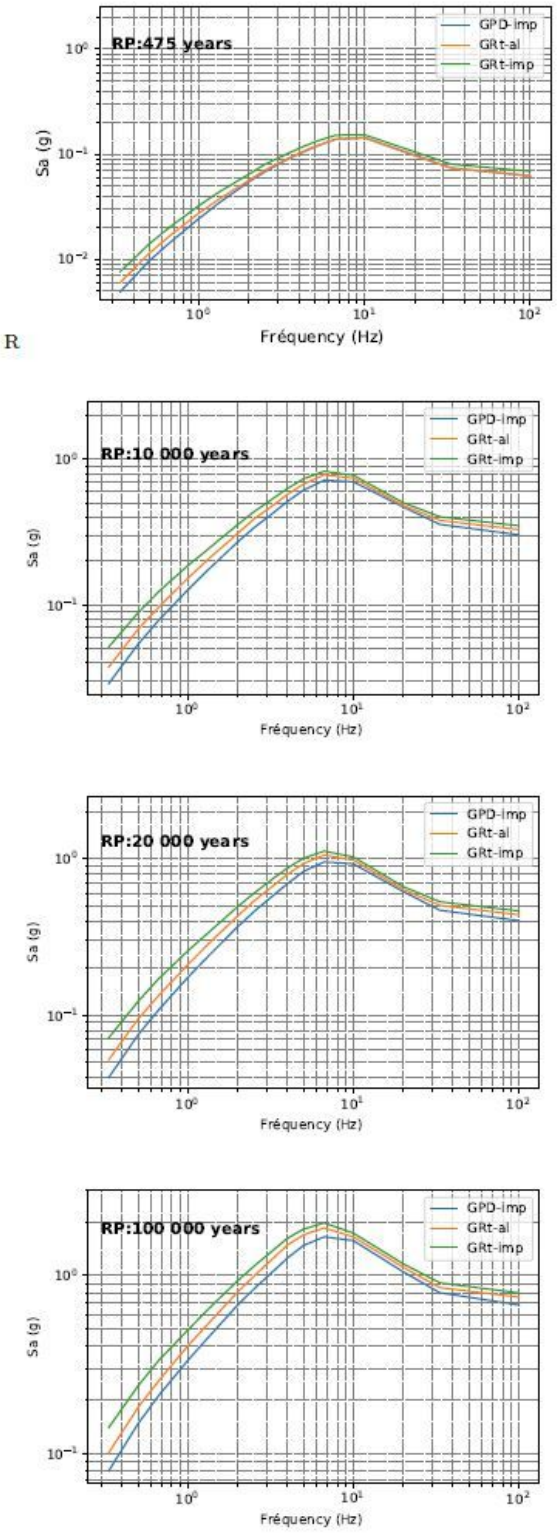

R

Figure 19

Comparison of the Uniform Hazard Spectra (UHS) between the new recurrence models: Random Gutenberg- Richter GRt-al, Generalized Pareto Distribution GPD-imp and the common Gutenberg-Richter model GRt-imp for the return periods (RP): 475, 10 000, 20 000 and 100 000 years.

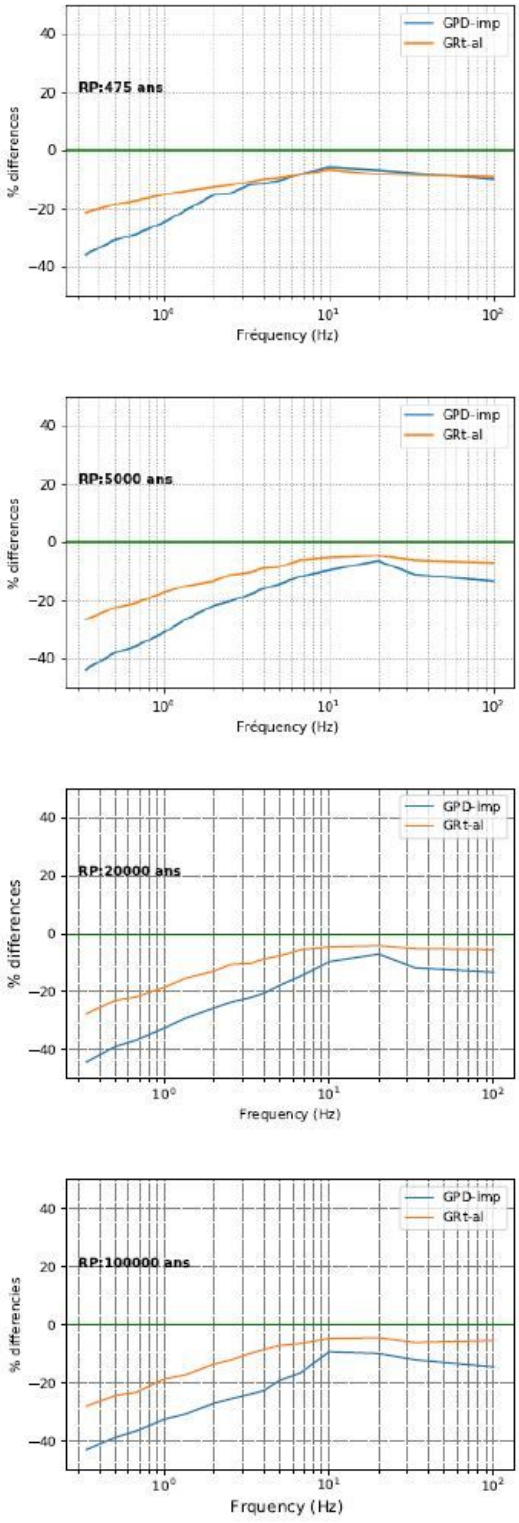

Figure 20

Relative differences of the UHS calculated with the new recurrence models (GPD-imp and GRt-al) with respect to the common Gutenberg Richter model (GRt-imp) considered as a reference.

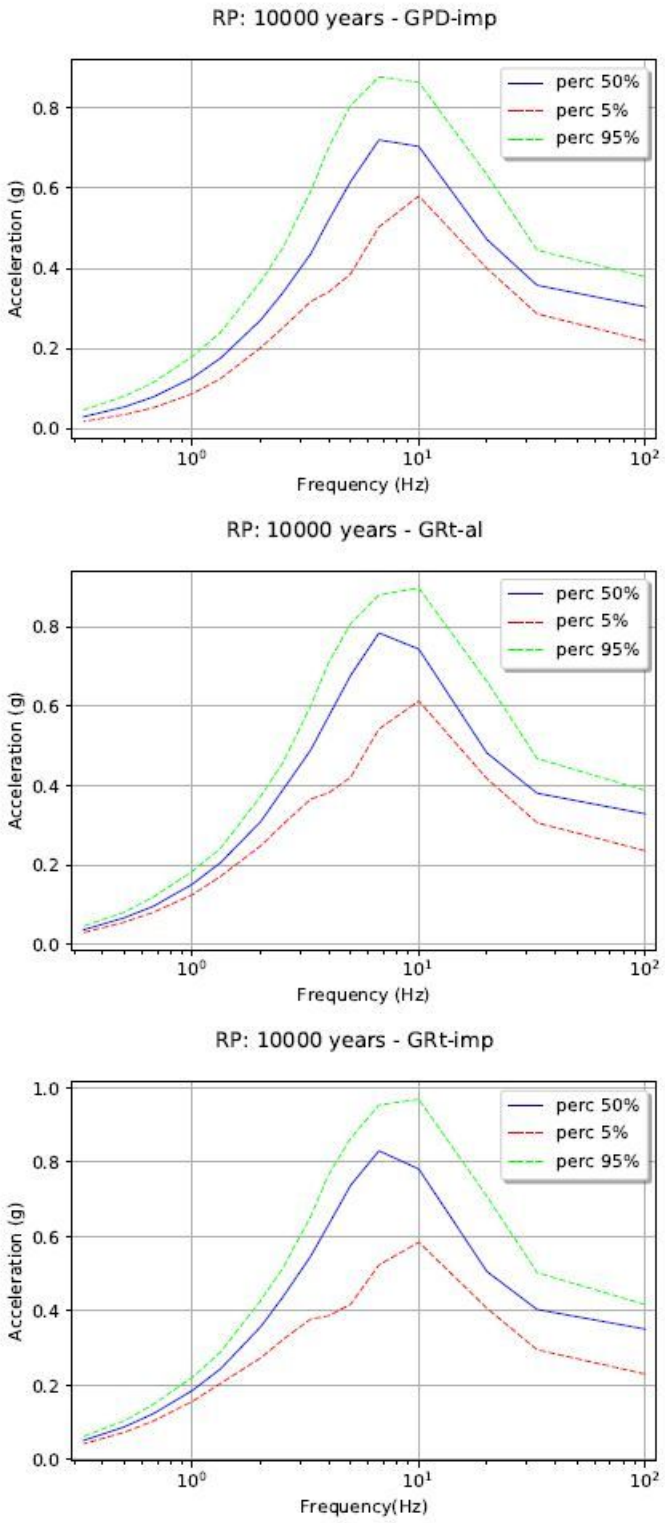

Figure 21

5%, 50% and 95% quantile curves of the UHS calculated with the new recurrence models (GPD-imp, GRt-al) and the common Gutenberg-Richter model GRt-imp.

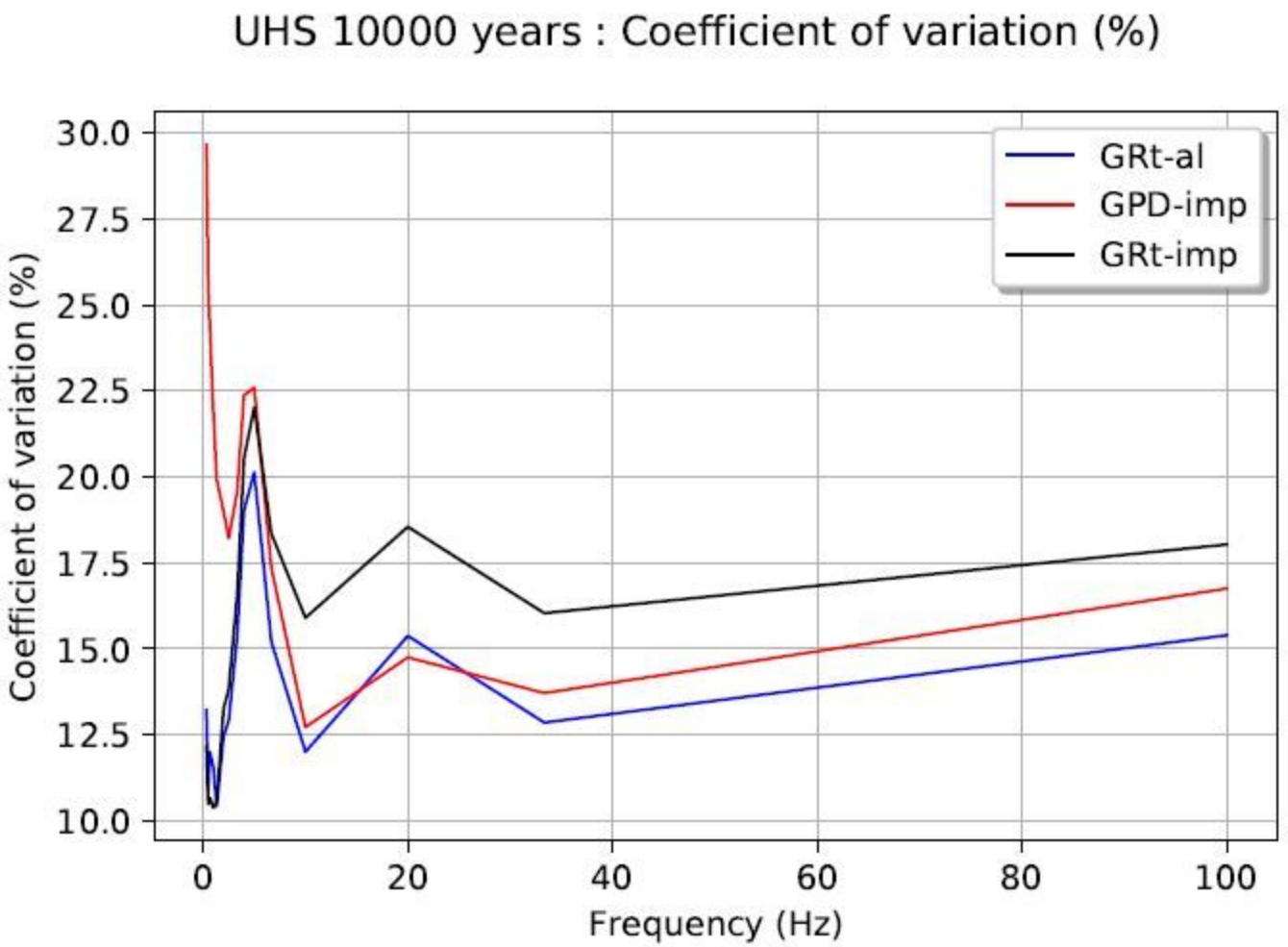

Figure 22

Uncertainties on parameters estimation: coefficient of variation of the UHS calculated with the recurrence models GPD-imp, GRt-al and the common Gutenberg-Richter model GRt-imp.